

Full length article

Prescribed burn related increases of population exposure to PM<sub>2.5</sub> and O<sub>3</sub> pollution in the southeastern US over 2013–2020

Kamal J. Maji, Zongrun Li, Yongtao Hu, Ambarish Vaidyanathan, Jennifer D. Stowell, Chad Milano, Gregory Wellenius, Patrick L. Kinney, Armistead G. Russell, M. Talat Odman



PII: S0160-4120(24)00687-1

DOI: <https://doi.org/10.1016/j.envint.2024.109101>

Reference: EI 109101

To appear in: *Environment International*

Received Date: 14 July 2024

Revised Date: 23 September 2024

Accepted Date: 24 October 2024

Please cite this article as: K.J. Maji, Z. Li, Y. Hu, A. Vaidyanathan, J.D. Stowell, C. Milano, G. Wellenius, P.L. Kinney, A.G. Russell, M. Talat Odman, Prescribed burn related increases of population exposure to PM<sub>2.5</sub> and O<sub>3</sub> pollution in the southeastern US over 2013–2020, *Environment International* (2024), doi: <https://doi.org/10.1016/j.envint.2024.109101>

This is a PDF file of an article that has undergone enhancements after acceptance, such as the addition of a cover page and metadata, and formatting for readability, but it is not yet the definitive version of record. This version will undergo additional copyediting, typesetting and review before it is published in its final form, but we are providing this version to give early visibility of the article. Please note that, during the production process, errors may be discovered which could affect the content, and all legal disclaimers that apply to the journal pertain.

## Prescribed Burn Related Increases of Population Exposure to PM<sub>2.5</sub> and O<sub>3</sub> Pollution in the Southeastern US over 2013–2020

Kamal J. Maji<sup>1</sup>, Zongrun Li<sup>1</sup>, Yongtao Hu<sup>1</sup>, Ambarish Vaidyanathan<sup>1</sup>, Jennifer D. Stowell<sup>2</sup>, Chad Milano<sup>2</sup>, Gregory Wellenius<sup>2</sup>, Patrick L. Kinney<sup>2</sup>, Armistead G. Russell<sup>1</sup>, and M. Talat Odman<sup>1,\*</sup>

<sup>1</sup> School of Civil and Environmental Engineering, Georgia Institute of Technology, Atlanta, Georgia 30332, USA

<sup>2</sup> School of Public Health, Boston University, Boston, Massachusetts 02118, USA

\*Corresponding author: talat.odman@ce.gatech.edu (M. Talat Odman)

### Abstract

Ambient air quality across the southeastern US has improved substantially in recent decades. However, emissions from prescribed burn remain high, which may pose a substantial health threat. We employed a multistage modeling framework to estimate year-round, long-term effects of prescribed burn on air quality and premature deaths. The framework integrates a chemical transport model with a data-fusion approach to estimate 24-h average PM<sub>2.5</sub> and maximum daily 8-h averaged O<sub>3</sub> (MDA8-O<sub>3</sub>) concentrations attributable to prescribed burn for the period 2013–2020. The Global Exposure Mortality Model and a log-linear exposure-response functions were used to estimate the premature deaths ascribed to long-term prescribed burn PM<sub>2.5</sub> and MDA8-O<sub>3</sub> exposure in ten southeastern states. Our results indicate that prescribed burn contributed on annual average  $0.59 \pm 0.20 \mu\text{g}/\text{m}^3$  of PM<sub>2.5</sub> ( $\sim 10\%$  of ambient PM<sub>2.5</sub>) over the ten southeastern states during the study period. On average around 15% of the state-level ambient PM<sub>2.5</sub> concentrations contributed by prescribed burn in Alabama ( $0.90 \pm 0.15 \mu\text{g}/\text{m}^3$ ), Florida ( $0.65 \pm 0.19 \mu\text{g}/\text{m}^3$ ), Georgia ( $0.91 \pm 0.19 \mu\text{g}/\text{m}^3$ ), Mississippi ( $0.65 \pm 0.10 \mu\text{g}/\text{m}^3$ ) and South Carolina ( $0.65 \pm 0.09 \mu\text{g}/\text{m}^3$ ). In the extensive burning season (January–April), daily average contributions to ambient PM<sub>2.5</sub> increased up to 22% in those states. A large part of Alabama and Georgia experiences  $\geq 3.5 \mu\text{g}/\text{m}^3$  prescribed burn PM<sub>2.5</sub> over 30 days/year. Additionally, prescribed burn is responsible for an average increase of  $0.32 \pm 0.12 \text{ ppb}$  of MDA8-O<sub>3</sub> ( $0.8\%$  of ambient MDA8-O<sub>3</sub>) over the ten southeastern states. The

combined effect of prescribed burn PM<sub>2.5</sub> exposure, population growth, and increase of baseline mortality over time resulted in a total of 20,416 (95% confidence interval (CI): 16,562–24,174) excess non-accidental premature deaths in the ten southeastern states, with 25% of these deaths in Georgia. Prescribed burn MDA8-O<sub>3</sub> was responsible for an additional 1,332 (95% CI: 858–1,803) premature deaths in the ten southeastern states. These findings indicate significant impacts from prescribed burn, suggesting potential benefits of enhanced forest management strategies.

**KEYWORDS:** southeastern US; prescribed burn; chemical transport model; air pollution; premature deaths

## 1. Introduction

Wildfires have been growing in size and frequency in the United States (US), paralleling the extension of the burn weather season, which is characterized by high temperatures and low humidity (Cunningham et al., 2024; Cromar et al., 2024; Xu et al., 2023). This trend, driven by climate change, has led to more severe burn weather conditions. Wildland burns—including both wildfires and prescribed burn account for 44% of the nation's primary emissions of fine particulate matter ( $PM_{2.5}$ ) in 2017, in which 32% are due to prescribed fire (USEPA, 2023a). However, in the Southeastern US, wildland burns contribute 31% of the primary  $PM_{2.5}$ , in which 81% are coming from prescribed fire (Cromar et al., 2024; D'Evelyn et al., 2022). The Environmental Protection Agency (EPA) recognizes the increasing challenges and human health impacts of wildland burns, and smoke pose in communities all around the country (USEPA, 2023a). Despite stringent controls and intensive monitoring of the country's vast forested areas (Burke et al., 2021), the annual acreage of forest land consumed by wildland burn in the US has doubled in past two decades (Burke et al., 2023). Controlled prescribed burn are effective in preventing destructive wildfires and typically emit less  $PM_{2.5}$  compared to wildfires of an equivalent burn area. Prescribed burn also supports ecosystem development, restoration, and management of wildland vegetation (Glassman et al., 2023).

Prescribed burns are low-intensity fires carried out under controlled environmental conditions to minimize the risk of uncontrolled spread and to enhance smoke dispersion before plumes affect downwind communities (Bajnath-Rodino et al., 2022; O'Dell et al., 2019). However, prescribed burns are conducted on a regular basis compared to wildfire events. Prescribed burns accounts for a significant portion of burn activity in the US, averaging 11 million acres per year. Of this, 70% occurs in the southeastern US (Kolden, 2019), where the primary fuels found in forests such as longleaf, slash, and loblolly pine forests with palmetto-gallberry understories in Florida, Georgia, and South Carolina, pine and mixed hardwood forests in the upper coastal plain of South Carolina, and shortleaf pine-grass assemblages in Arkansas (Prichard et al., 2017; Reid et al., 2012; Wright, 2013). The annual rate of increase of burn area approximately 0.15 million acres in the southeastern US (Burke et al., 2023; Kondo et al., 2022). In the southeastern US, prescribed burn contributes about 10–15% to the annual average ambient  $PM_{2.5}$  levels, which can rise to 20–30% during the extensive burning season (January–April) (Afrin and Garcia-Menendez, 2020; Carter et al., 2023).

The contribution of prescribed burn to regional ambient air pollution may offset the air quality improvements achieved in the US over the past few decades. Consequently, emissions from prescribed burns are classified as exceptional event pollutants and are not included in ambient air quality standards (USEPA, 2019). Previous studies estimating the contribution of prescribed burns to ambient air pollution have primarily focused on  $PM_{2.5}$  impacts, often overlooking their contribution to ozone ( $O_3$ ) pollution. Furthermore, these estimates are confined to the extensive prescribed burning season and not provided a complete year-long picture. Additionally, long-term exposure to air pollution poses a greater human health risk; however, only a few long-term health impact assessment studies have been conducted to quantify the premature deaths attributed to prescribed burn pollution. This gap is primarily due to the challenges in estimating long-term prescribed burn smoke exposure with high spatial and temporal resolutions (Zhang et al., 2023). The absence of a comprehensive assessment of the impacts of prescribed burn on both regional

and local air pollution levels hinders the development of evidence-based policies. Such policies are necessary for using prescribed burn as an effective tool in land management.

To address the evidence gap regarding the impacts of prescribed burn on air quality, we leveraged recent advancements in chemical transport modeling, the availability of remote sensing data, and statistical methods. Our aim was to estimate the effects of prescribed burn on regional and local PM<sub>2.5</sub> and O<sub>3</sub> levels across the southeastern US. Additionally, for contextual understanding, we employed a standard health impact assessment approach to estimate the excess deaths attributable to the increased levels of PM<sub>2.5</sub> and O<sub>3</sub> resulting from prescribed burn.

## 2. Materials and Methods

We designed a multistage modeling framework to estimate year-around prescribed burn impacts on air quality and health in ten southeastern US states (i.e., Alabama, Florida, Georgia, Kentucky, Mississippi, North Carolina, South Carolina, Tennessee, Virginia and West Virginia) from 2013 to 2020. This framework consists of: (a) identification of daily prescribed burn information from the satellite-derived product Burn INventory from NCAR (FINN); (b) simulation of prescribed burn contributions to 24-h average PM<sub>2.5</sub> and daily maximum 8-h average O<sub>3</sub> (MDA8-O<sub>3</sub>) using the Community Multiscale Air Quality (CMAQ) model; (c) data-fusion to integrating CMAQ simulated PM<sub>2.5</sub> and MDA8-O<sub>3</sub> with daily observations to reduce model uncertainty; and (d) health impact assessment to estimate excess premature deaths associated with the change in PM<sub>2.5</sub> and MDA8-O<sub>3</sub> exposure due to prescribed burn (Figure S1).

### 2.1. Prescribed burn identification and emissions.

The permit records often provide more precise measurements of burned areas compared to satellite data, however a complete record of prescribed burn in southeastern states is not available. Additionally, the information contained in burn permit records, such as location, date and time, may sometimes be incorrect, leading to potential misidentification of burn locations and sizes (Afrin and Garcia-Menendez, 2020; Jaffe et al., 2020). We bridged this data gap by using FINN burn area data (version 2.5), a high-resolution satellite-based remote sensing product. FINN utilizes MODIS and VIIRS active burn data derived from thermal anomalies and combines them with land cover data to estimate daily burn area and emissions (Li et al., 2020). However, FINN does not distinguish between prescribed burn, wildfires, or agricultural burns. In our study, we utilized the prescribed burn data provided by Li et al. (2023). In that study, they implemented a burn-type differentiation algorithm to distinguish the types of fire in FINN. The algorithm utilizes the NLCD land use data to identify fires on agricultural lands as agricultural burns and employs a spatiotemporal clustering algorithm to estimate the durations of remaining fires. Then, it assumes that fires that last one day are prescribed burns and those that last longer are wildfires. Since permit records provide more precise measurements of burned areas, we employed a linear regression model to calibrate the FINN-based burned area data. This calibration was done using available permit records in Florida, Georgia and South Carolina, hoping to enhance the accuracy of burned area information over the entire domain. However, note that these permit burn area records can also contain inaccuracies, such as underreported/overreported (Huang et al., 2018) and that the three states mentioned above may not represent the rest of the Southeastern US. In addition to burned areas, FINN also provides fire emissions; however, instead of using those estimates we

chose to recalculate the emissions using the adjusted burned areas described above in the BlueSky smoke modeling framework (Michael et al., 2023). There were several reasons for this decision. First, while FINN uses a more generalized classification for the fuels because of its global nature, BlueSky utilizes a more detailed classification that is customized for the fuels in the US. Second, BlueSky considers the meteorological conditions and fuel moistures to calculate the amounts of fuels consumed while FINN infers consumptions from fire radiative power (Ottmar et al., 2007). Third, the emission factors in BlueSky were recently updated with the most up to date information (Prichard et al., 2020a). Note that despite all these differences in methodology, we found a high correlation and strong agreement between the daily total emissions calculated using BlueSky and those from FINN (Li et al., 2023). Finally, FINN emissions are daily and two-dimensional, but air quality models require hourly and three-dimensional emission inputs. Bluesky is equipped with empirical time profiles that differentiate between wildfires and prescribed burns and plume-rise schemes that have been tested with data from prescribed fire experiments (Liu, 2014).

## 2.2. Air quality model configurations.

Our air quality modeling system consisted of the Weather Research and Forecasting Model (WRF; version 3.9), a numerical weather prediction model, and CMAQ (version 5.3), a chemical transport model (CTM). CMAQ combines emission and weather inputs and models atmospheric transport, dispersion, chemical transformation, and deposition processes to simulate hourly pollution levels (Appel et al., 2021). The meteorological inputs to CMAQ were developed using the Weather Research and Forecasting (WRF) model version 3.9.1.1 (Skamarock et al., 2008) with NAM analysis and ADP observational datasets (Hu et al., 2022). The WRF model was configured with the RRTMG scheme for radiation, the Kain-Fritsch scheme for cumulus parameterization, the Morrison (2 moments) scheme for microphysics, the ACM2 Planetary Boundary Layer (PBL) scheme and the Pleim-Xiu Land Surface Model (LSM). We used the Carbon Bond 6 (CB6) gas phase chemistry mechanism and the AERO6 aerosol module in CMAQ. Our modeling domain, shown in Figure S2, had a horizontal resolution of 12 km×12 km, covering the southeastern US (29.41 to 41.78°N and -90.36 to -70.91°W) with 123x138 grid cells. We used the National Emission Inventory (NEI) for all anthropogenic emissions other than prescribed burn emissions. As for natural emissions, we used the Biogenic Emission Inventory System, version 4 (BEIS4) for biogenic emissions and the built-in windblown dust and sea spray aerosol emissions in CMAQ. To quantify the prescribed burn impacts, we generated two sets of concentration fields from two CMAQ simulations between January 2013 and December 2020: a baseline simulation with all emissions ( $C_{all}^s$ ) and a second simulation excluding prescribed burn emissions ( $C_{no-PB}^s$ ). We then calculated the prescribed burn contributed pollution as:

$$\Delta C_{PB}^s(x,t) = C_{all}^s(x,t) - C_{no-PB}^s(x,t) \quad (1)$$

where superscript  $s$  indicates simulated concentration and  $x$  and  $t$  denote space and time variability.

## 2.3. Data fusion method:

Modeled concentrations have uncertainties related to emissions inputs, meteorological parameters, and physical/chemical transport processes; therefore, they differ from in-situ measurements (Friberg et al., 2016; Senthilkumar et al., 2019). To reduce the model biases and error, we followed

Friberg et al. (2016) and fused observational data from fixed air quality monitors with daily average PM<sub>2.5</sub> and MDA8-O<sub>3</sub> fields simulated by CMAQ. Across eight years of observations at 252 PM<sub>2.5</sub> and 258 O<sub>3</sub> monitors in the study area, with 437 thousand PM<sub>2.5</sub> and 513 thousand MDA8-O<sub>3</sub> daily observations were obtained from EPA-AQS (Environmental Protection Agency-Air Quality System). The data-fused concentration fields ( $C_{all}^p$ ) are produced for pollutant  $p$  by a regression model as described in Maji et al. (2024).

Finally, observation-adjusted no-prescribed burn concentration ( $AdjC_{no-PB}^p$ ) and observation-adjusted prescribed burn impact ( $\Delta AdjC_{PB}^p$ ) fields were generated as follows:

$$AdjC_{no-PB}^p(x,t) = C_{no-PB}^s(x,t) \times [C_{all}^p(x,t)/C_{all}^s(x,t)] \quad (3)$$

$$\Delta AdjC_{PB}^p(x,t) = \Delta C_{PB}^s(x,t) \times [C_{all}^p(x,t)/C_{all}^s(x,t)] \quad (4)$$

#### 2.4. Premature deaths assessment:

The calculation of excess deaths attributable to long-term exposure to pollutant  $p$  from prescribed burn smoke within grid cell ( $x$ ) at time ( $t$ ) follows a well-established method to estimate air pollution related mortality (Anenberg et al., 2010; Neumann et al., 2021):

$$\Delta M_{PB}^p(x,t) = \sum_{d,a} [AF_{d,a, \overline{C_{all}^p}(x,t)} - AF_{d,a, \overline{AdjC_{no-PB}^p}(x,t)}] \times B_{d,a}(x,t) \times Pop_a(x,t) \quad (5)$$

where  $d$  represents a specific disease (e.g., stroke, lung cancer etc.) while  $a$  denotes specific age group,  $AF$  is the attributable fraction at annual average concentration level, and  $B_{d,a}(x,t) \times Pop_a(x,t)$  is the of total disease-specific '*Reported Mortality*'. Since mortality is typically recorded at the state or county-level, however as county-level baseline value for all disease are not available, a common approach to estimate baseline mortality at the grid cell level is to scale the reported mortality to the grid cell population ( $Pop_a$ ) data by using the baseline mortality rate ( $B_{d,a} = Report Mortality_{d,a}/Pop_a$ ) at state levels. State-level mortality is obtained by the sum of  $\Delta M_{PB}^p(x,t)$  for each grid cell in a state within the study domain.  $AF$  can be estimated for each age group  $a$  and disease  $d$  as:

$$AF_{d,a,\overline{C^p}} = (1 - RR_{d,a}(\overline{C^p})) / RR_{d,a}(\overline{C^p}) \quad (6)$$

with  $RR_{d,a}(\overline{C^p})$  being the relative risk (or hazard ratio) for pollutant  $p$  at the annual average concentration level  $\overline{C^p}$ .

We recognize that the mortality risk associated with chronic exposure to prescribed burn PM<sub>2.5</sub> may differ from that linked to all-source PM<sub>2.5</sub>. However, since there is a lack of specific studies addressing the increased mortality risk from chronic exposure to prescribed burn PM<sub>2.5</sub> we opted to use the Global Exposure Mortality Model (GEMM) as a practical approach to estimate premature deaths attributable to chronic exposure (Burnett et al., 2018). Our method involved two GEMM modules: the GEMM-NCD+LRI module to estimate non-accidental deaths [predominantly due to noncommunicable diseases (NCDs) and lower respiratory infections (LRIs)], and the GEMM-5COD model to calculate five types of disease-specific deaths [(ischemic

heart disease (IHD), stroke (CEV), chronic obstructive pulmonary disease (COPD), lung cancer (LC), and lower respiratory tract infections (LRI)]. For comparison, we also estimated these five disease-specific deaths using the Integrated Exposure Response (IER) model (Burnett et al., 2014). Additionally, to estimate all-cause mortality attributed to prescribed burn MDA8-O<sub>3</sub> exposure, we employed a log-linear concentration response function (CRF) (Maji et al., 2023; Pozzer et al., 2023; Sun et al., 2022). The disease-specific and state-specific baseline mortality for age group  $\geq 25$  years were obtained from the Global Burden of Disease (GBD) results tool (IHME, 2019). The spatial distribution of the population with 1 km<sup>2</sup> resolution is taken from the Gridded Population of the World (GPW) dataset (WorldPop, 2023) and mapped on our 12-km CAMQ resolution grid.

### 3. Results and Discussion

The prescribed burn area exhibited high variation across different states. Prescribed burn constituted an estimated 79% of the total number of burns in Alabama, 76% in South Carolina, and 66% in Georgia. Between 2013 to 2020, 25.1 million acres ( $\sim 3$  million acres/year) of land were treated as prescribed burn in the study domain (Figure 1 and Figure S3), in which about 55% area burn during the extensive burning season (4 months), while 21 and 24% area burn during low burn season (5 months) and moderate burn season (3 months), respectively. Of the total prescribed burn area, 83.7% on private lands with the rest on federal lands (Figure S4 to S6). The seasonal patterns of prescribed burns on federal and private lands show similar trends, with the most intense burning activity occurring between January and May. Prescribed burning contributed to emissions of about 3.28 million tons of PM<sub>2.5</sub>, 3.50 million tons of volatile organic compounds (VOCs), and 0.37 million tons of nitrogen oxides (NO<sub>x</sub>), during the study period. The years 2014 and 2017 saw larger total burn area, 3.55 and 3.74 million acres respectively, and emissions accounting for about 30% of total prescribed burn emissions during these two years (Figures S7-S9 and Table S2). The year-to-year differences are due to meteorological conditions (some years have more favorable weather for burning), policy and management practices (e.g., there were more burns in 2017 in the wake of wildfires in the Southern Appalachian Mountains) and programmatic support and funding (fire management funding can fluctuate from year to year) (Melvin, 2018; Boby et al., 2023).

**Figure 1.** Spatial distribution of total prescribed burned area from adjusted-FINN (top) and corresponding total emissions of PM<sub>2.5</sub>, VOCs and NO<sub>x</sub> (bottom) during 2013–2020 (unit is acres for burned area and tons for PM<sub>2.5</sub>, VOCs and NO<sub>x</sub>) emissions.

#### 3.1. Assessing Model Performance

Model evaluation indicated that CMAQ generally underestimated PM<sub>2.5</sub> (by  $\sim 21\%$ ) and overestimated MDA8-O<sub>3</sub> (by  $\sim 23\%$ ) with respect to EPA measurement over the study period in ten southeastern states. Data-fusion reduced PM<sub>2.5</sub> underestimation to 0.6% and MDA8-O<sub>3</sub> overestimation to 0.3%. R<sup>2</sup> over the study domain was 0.65 (root mean squared error (RMSE) = 3.04 µg/m<sup>3</sup>; normalized mean error (NME) = 24%, normalized mean bias (NMB) = -10%) for PM<sub>2.5</sub>, and 0.86 (RMSE = 4.29 ppb; NME = 8%, NMB = -1.5%) for MDA8-O<sub>3</sub>, (Figure S10 and

Table S3), above typical values for fields developed using only CTMs (Emery et al., 2017) and satellite-based PM<sub>2.5</sub> data (van Donkelaar et al., 2010).

The data-fusion method performance was also evaluated using a comprehensive 10-fold cross-validation analysis. The results (Table S3) indicated data-fusion performed better compared to CMAQ simulation, with larger R<sup>2</sup> and smaller MB, RMSE and NMB when compared to EPA monitor data. All performance metrics for PM<sub>2.5</sub> (R<sup>2</sup>=0.64, MB= -0.39 µg/m<sup>3</sup>, RMSE = 3.53 µg/m<sup>3</sup>, NMB = -4.69%), and MDA8-O<sub>3</sub> (R<sup>2</sup>=0.82, MB= -1.73 ppb, RMSE = 4.18 ppb, NMB = -4.36%) met the criteria and goals for CTMs (Emery et al., 2017). While data-fusion showed improved statistical performance, potential biases may exist due to the inherent limitations of both data-fusion and EPA data's ground truthing.

### 3.2. Impacts on Air Quality

The study measured the contribution of prescribed burn to annual and seasonal PM<sub>2.5</sub> and MDA8-O<sub>3</sub> levels by aggregating daily data across the ten southeastern states and individual states. The simulated annual mean prescribed burn PM<sub>2.5</sub> and MDA8-O<sub>3</sub> show significant temporal and spatial variation, in alignment with the burned areas (Figure 2 and Figure 3). The locations with the highest annual average PM<sub>2.5</sub> levels ( $\geq 1.4 \text{ } \mu\text{g}/\text{m}^3$ ) from prescribed burns are associated with areas of extensive prescribed burning, with impacts often extending across large regions. These hotspot locations vary annually based on the extent of the burned area, as prescribed burns are typically repeated every two to three years. However, they are primarily concentrated along the Alabama-Georgia border. Certain grids experienced daily PM<sub>2.5</sub> levels of around 46 µg/m<sup>3</sup> and MDA8-O<sub>3</sub> levels of 55 ppb from prescribed burn (Figure S11).

**Figure 2.** Spatial distributions of yearly average prescribed burn specific PM<sub>2.5</sub> concentrations ( $\mu\text{g}/\text{m}^3$ ) during 2013–2020.

**Figure 3.** Spatial distributions of yearly average prescribed burn specific MDA8-O<sub>3</sub> concentrations (ppb) during 2013–2020.

On average, prescribed burn contributed  $0.59 \pm 0.20 \text{ } \mu\text{g}/\text{m}^3$  of PM<sub>2.5</sub> across the ten southeastern states during 2013–2020, accounting for ~10% of the ambient PM<sub>2.5</sub>. At the state-level, contribution of average prescribed burn PM<sub>2.5</sub> was considerably higher in Alabama [ $0.90 \pm 0.15$  ( $0.91$ ) µg/m<sup>3</sup>], Florida [ $0.65 \pm 0.19$  ( $0.64$ ) µg/m<sup>3</sup>], Georgia [ $0.91 \pm 0.19$  ( $0.91$ ) µg/m<sup>3</sup>], Mississippi [ $0.65 \pm 0.1$  ( $0.64$ ) µg/m<sup>3</sup>], and South Carolina [ $0.65 \pm 0.09$  ( $0.65$ ) µg/m<sup>3</sup>] [mean±SD (median)], compared to domain average (Figure 4). These levels accounted for approximately 15% of ambient PM<sub>2.5</sub> in each respective state. In other states, the contribution of prescribed burn to ambient PM<sub>2.5</sub> was less than 6%. Notably, Alabama and Georgia recorded the highest annual average level of PM<sub>2.5</sub> contribution from prescribed burn, exceeding 1.0 µg/m<sup>3</sup> in 2015 and 2017 (Table A.1). The highest annual average prescribed burn PM<sub>2.5</sub> were recorded in Chattahoochee and Marion

Counties (central Georgia), and Russell County (southeastern Alabama), reaching an average of  $1.20 \mu\text{g}/\text{m}^3$  during 2013–2020 (Figure S12).

**Figure 4.** Boxplot of state-specific prescribed burn contributed daily average PM<sub>2.5</sub> (top) and daily MDA8-O<sub>3</sub> (bottom) from 2013–2020. The top and bottom of the box indicate the 75<sup>th</sup> and 25<sup>th</sup> percentile of yearly values. The vertical solid lines indicate the interquartile range of yearly values. The horizontal blue line is the annual mean, and the top and bottom pink stars indicate the 95<sup>th</sup> and 5<sup>th</sup> percentile of yearly values. The long black horizontal line indicates the average prescribed burn PM<sub>2.5</sub> and MDA8-O<sub>3</sub> over the ten southeastern states from 2013–2020.

During the extensive burning season from 2013 to 2020, the average contribution of prescribed burn PM<sub>2.5</sub> was higher in Alabama [ $1.15 \pm 0.26$  ( $1.13$ )  $\mu\text{g}/\text{m}^3$ ], Georgia [ $1.41 \pm 0.36$  ( $1.40$ )  $\mu\text{g}/\text{m}^3$ ], and South Carolina [ $1.05 \pm 0.15$  ( $1.03$ )  $\mu\text{g}/\text{m}^3$ ] (Figure 5 and Table S4). In these states, prescribed burn contributed over 75% to total daily PM<sub>2.5</sub> on the days with highest burn area, compared to an average of 22% during the extensive burning season. For example, on March 23, 2016, when the highest burned area was reported as 63,710 acres, prescribed burn contributed around  $9.0 \mu\text{g}/\text{m}^3$  of PM<sub>2.5</sub> in Georgia, North Carolina, South Carolina, and Virginia, comprising approximately 75% of the ambient PM<sub>2.5</sub> (Figure S14). In 2017 extensive burning season, the average prescribed burn PM<sub>2.5</sub> was  $2.05 \pm 0.57$  ( $2.11$ )  $\mu\text{g}/\text{m}^3$  in Georgia, highest among all states. During the moderate burning season (October–December), we observed that the contribution of prescribed burn to PM<sub>2.5</sub> was higher than the annual average in all states, with particularly significant contributions in Alabama [ $1.19 \pm 0.18$  ( $1.21$ )  $\mu\text{g}/\text{m}^3$ ], Georgia [ $1.00 \pm 0.23$  ( $1.02$ )  $\mu\text{g}/\text{m}^3$ ], and Mississippi [ $0.93 \pm 0.15$  ( $0.93$ )  $\mu\text{g}/\text{m}^3$ ]. These levels accounted for approximately 20% of the ambient PM<sub>2.5</sub> in each respective state during this period (Figure 5). Notably, in Mississippi and Tennessee, the prescribed burn PM<sub>2.5</sub> levels during October–December consistently surpassed the levels during the January–April. This trend may be attributed to those states' practice of conducting a majority of their prescribed burn in the October–December season (Table S6).

From 2013 to 2020, prescribed burn contributed to an average increase of  $0.33 \pm 0.12$  ppb in MDA8-O<sub>3</sub> levels across the ten southeastern states, representing ~0.8% of the ambient MDA8-O<sub>3</sub>. At state-level, prescribed burn was responsible for an average increase in MDA8-O<sub>3</sub> by  $0.42 \pm 0.09$  ( $0.40$ ) ppb in Alabama,  $0.46 \pm 0.12$  ( $0.44$ ) ppb in Florida,  $0.51 \pm 0.13$  ( $0.51$ ) ppb in Georgia, and  $0.36 \pm 0.05$  ( $0.35$ ) ppb in South Carolina, accounting for about 1.0% of ambient MDA8-O<sub>3</sub> (Table 2). The highest prescribed burn contributions to MDA8-O<sub>3</sub> were observed in Thomas and Grady Counties (in southwestern Georgia) and Gadsden County (in northwestern Florida), reaching average 1.00 ppb during the study period. The counties with elevated MDA8-O<sub>3</sub> levels are approximately 180 km away from the counties with high-levels of prescribed burn PM<sub>2.5</sub>. This is because PM<sub>2.5</sub> peaks primarily due to burn emissions, while O<sub>3</sub> is formed during transport, with peak concentrations occurring farther away, influenced by meteorological conditions.

During the extensive burning season, the contribution of prescribed burn to MDA8-O<sub>3</sub> is higher ( $0.56\pm0.23$  ppb), accounting for ~2.2% of ambient MDA8-O<sub>3</sub> (Table S7). Similar to the highest contribution of daily average prescribed burn PM<sub>2.5</sub>, high MDA8-O<sub>3</sub> levels were also recorded on days with the largest areas burned. For instance, on March 23, 2016, prescribed burn was responsible for an increase of around 3.5 ppb MDA8-O<sub>3</sub> in Georgia, North Carolina, South Carolina, and Virginia, which was about 8% of the ambient MDA8-O<sub>3</sub> (Figure S13 and S14). During the moderate burning season, we noted that prescribed burn MDA8-O<sub>3</sub> levels were comparatively lower than those observed during the extensive burning season. However, the average contributions in Alabama [ $0.49\pm0.10$  (0.47) ppb], Florida [ $0.40\pm0.10$  (0.40) ppb], and Georgia [ $0.49\pm0.12$  (0.49) ppb] were still noteworthy. These contributions accounting for approximately 1% of the ambient MDA8-O<sub>3</sub> in these states are notable especially since the winter period is generally less favorable for O<sub>3</sub> formation (Table S9). During the summer (May–September), ozone-season restrictions on certain open burning activities lead to a reduction in prescribed burn contributions to PM<sub>2.5</sub> and MDA8-O<sub>3</sub>, although some understory prescribed burn still contribute very low-levels (Table S5 and Table S8).

In 2020, in Alabama Georgia, Kentucky and Mississippi, prescribed burn PM<sub>2.5</sub> and MDA8-O<sub>3</sub> levels were higher during the moderate burning season compared to the extensive burning season. This shift might be linked to COVID-19 lockdown restriction or higher-than-usual rainfall during the extensive burn season (NOAA, 2020). As a result, most prescribed burning plan was rescheduled from January–April to October–December, leading to a 10% higher prescribed burn area in moderate burn season.

**Figure 5.** Spatial distributions of seasonal average prescribed burn specific PM<sub>2.5</sub> ( $\mu\text{g}/\text{m}^3$ ) (top) and MDA8-O<sub>3</sub> concentrations (ppb) (bottom) during 2013–2020. January–April is the extensive burning season, May–September is the low burning season and October–December is the moderate burning season.

### 3.3. Impact of Prescribed Burn on Air Quality Relative to NAAQS

We assessed the impact of prescribed burn relative to the national ambient air quality standards (NAAQS). We defined a prescribed burn ‘smoke-day’ as when prescribed burn contributed  $\geq 10\%$  of NAAQS, i.e.,  $\geq 3.5 \mu\text{g}/\text{m}^3$  to ambient daily average PM<sub>2.5</sub> concentration (NAAQS:  $35 \mu\text{g}/\text{m}^3$ ) and  $\geq 7$  ppb to ambient MDA8-O<sub>3</sub> (NAAQS: 70 ppb). Out of 252 AQS monitoring sites, 22 (~9%) experienced over 15 smoke-days/year and 46 sites (~18%) experienced over 10 smoke-days/year due to prescribed burn PM<sub>2.5</sub>. In 2017, the year with the highest burn area, 33 sites primarily located in Georgia, Alabama and South Carolina (Figure S15) experienced at least 20 smoke-days, indicating a hotspot location for the impact of prescribed burn PM<sub>2.5</sub> in the southeastern US. Among these 33 sites, the distance to the nearest burn location ranged from 914 meters to 11,931 meters. The impact of prescribed burn on air quality was highest during the extensive burning season, with 15 sites in Georgia significantly affected ( $\geq 15$  smoke-days/year) by prescribed burn.

Over the eight years of the study, only 11 sites, located in southwestern Georgia and northwestern Florida, experienced more than 20 smoke-days due to prescribed burn MDA8-O<sub>3</sub>.

During the study period, we observed significant contributions of prescribed burn to the PM<sub>2.5</sub> levels in several states: 89 smoke-days in Alabama, 158 in Georgia, 112 in Tennessee, 91 in North Carolina, and 72 in South Carolina. In terms of MDA8-O<sub>3</sub> levels, there were 67 smoke-days in Alabama, 67 in Georgia, 86 in North Carolina, and 83 in South Carolina. At grid-level, we observed large parts of Alabama and Georgia experiencing over 240 smoke-days (on average 30 days/year) due to prescribed burn PM<sub>2.5</sub> and a significant portion of Georgia and Florida experiencing over 40 smoke-days (on average 5 days/year) due to prescribed burn MDA8-O<sub>3</sub> (Figure 6 and S16).

**Figure 6.** Distributions of the total smoke-days due to prescribed burn PM<sub>2.5</sub> (left) and MDA8-O<sub>3</sub> (right) during 2013–2020. We defined a prescribed burn smoke-day as when prescribed burn smoke contributed  $\geq 10\%$  of NAAQS, i.e.,  $\geq 3.5 \text{ } \mu\text{g}/\text{m}^3$  to 24-hr average PM<sub>2.5</sub> mass concentration (NAAQS is 35  $\mu\text{g}/\text{m}^3$ ) and  $\geq 7 \text{ ppb}$  to MDA8-O<sub>3</sub> (NAAQS is 70 ppb).

### 3.4. Impact on Excess Premature Deaths

Our analysis indicates that premature deaths due to prescribed burn-related smoke exposure are influenced by various factors, including the area burned, population dynamics and state-level baseline mortality over time. In the ten southeastern states under study, with a population of 62 million, the average population-weighted exposures to prescribed burn PM<sub>2.5</sub> and MDA8-O<sub>3</sub> were 0.61  $\mu\text{g}/\text{m}^3$  and 0.31 ppb, respectively. The average population-weighted exposures were notably higher in Alabama (0.88  $\mu\text{g}/\text{m}^3$  and 0.38 ppb) and Georgia (0.88  $\mu\text{g}/\text{m}^3$  and 0.46 ppb). The highest population-weighted exposure to prescribed burn PM<sub>2.5</sub> occurred in 2017 across the ten southeastern states, with an average of 0.75  $\mu\text{g}/\text{m}^3$ . Alabama and Georgia experienced even higher levels in 2017, at 1.04  $\mu\text{g}/\text{m}^3$  and 1.15  $\mu\text{g}/\text{m}^3$ , respectively. Conversely, the highest population-weighted exposure to prescribed burn MDA8-O<sub>3</sub> was found in 2014, averaging 0.41 ppb across the ten southeastern states, with peak levels of 0.62 ppb in Florida and 0.60 ppb in Georgia. It is important to note that these population-weighted values are lower than the annual average prescribed burn contributed pollution concentrations, largely because the burn areas are typically situated away from densely populated regions.

Across the ten states from 2013–2020, the total excess non-accidental premature deaths attributed to prescribed burn PM<sub>2.5</sub>, as estimated using the GEMM-NCD+LRI model, was 20,416 (95% confidence interval (CI): 16,562–24,174). This accounted for 10.4% of the total non-accidental premature mortality attributable to ambient PM<sub>2.5</sub>. For comparison, using the GEMM-5COD model, the total five-cause specific premature death was 13,642 (95% CI: 9,343–17,709), and using the IER model, it was 8,611 (95% CI: 3,669–11,318) for the same period. Previously unaccounted non-communicable diseases (other-NCD) (GEMM-NCD+LRI minus GEMM-5COD) connected to 6,774 (33%) premature deaths from prescribed burn PM<sub>2.5</sub>. Ischemic heart

disease (IHD) was the biggest cause of premature death, accounting for 42% in the GEMM-5COD model and 39% in the IER model (Table S2). The year 2017 witnessed the highest number of prescribed burns PM<sub>2.5</sub>-attributed non-accidental premature deaths [3,397 (95% CI: 2,753–4,025)], a consequence of the highest burn area and associated increased exposure to prescribed burn PM<sub>2.5</sub> (Table 3). In terms of regional impact during 2013–2020, Georgia accounted for 24% of the total excess non-accidental premature deaths [4,974 (95% CI: 4,036–5,887)], followed by North Carolina with 16% [3,229 (95% CI: 2,620–3,822)], and Alabama with 12% [2,454 (95% CI: 1,991–2,906)].

During 2013–2020, prescribed burn MDA8-O<sub>3</sub> attributed long-term exposure was responsible for an estimated 1,332 (95% CI: 858–1,803) excess all-cause premature deaths across the ten states. This accounted for 2.6% of the total ambient MDA8-O<sub>3</sub> attributed all-cause premature mortality. Of these excess all-cause deaths, Georgia and North Carolina accounted for significant portions, with 334 (95% CI: 216–453) and 210 (95% CI: 136–285) deaths, respectively. The highest number of all-cause deaths attributable to prescribed burn MDA8-O<sub>3</sub> exposure was estimated in 2014 and 2017, with 209 premature deaths. Notably, the instances of high premature deaths were predominantly in regions of higher population density, in contrast to the areas with elevated concentrations of prescribed burn smoke (Figure 7).

**Figure 7.** Distributions of premature mortality due to prescribed burn smoke PM<sub>2.5</sub> exposure (left) and MDA8-O<sub>3</sub> exposure (right) at the gridded-level (12 km<sup>2</sup>). The estimates of premature mortality are reported as the sum of annual values over 2013–2020. The concentration-response relationship from GEMM-NCD+LRI was used for PM<sub>2.5</sub> and Sun et al. (2022) study for MDA8-O<sub>3</sub>.

### 3.5. Limitations, Knowledge Gap and Future Study

This study utilized a unique clustering algorithm to identify prescribed burn information from the satellite-based fire product, applied a CTM followed by data-fusion to assess the contribution of prescribed burn to air quality, and performed a 10-fold cross-validation for model performance evaluation. It also explored potential premature death impacts of prescribed burn-related pollutions exposure in the southeastern US using well-established methods, as well as a sensitivity analysis assessing PM<sub>2.5</sub>-associated mortality using various CRF models. However, the study faced three major uncertainties and limitations: (1) reliance on satellites to identify prescribed burn; (2) potential overestimation or underestimation of emissions by the BlueSky model, and (3) the assumption of equal risks for prescribed burn-specific PM<sub>2.5</sub> and PM<sub>2.5</sub> from all other sources.

We utilized the FINN data for daily burn area and burn location information, which is based on thermal anomalies detected by MODIS and VIIRS satellites (Wiedinmyer et al., 2023). A significant drawback of this thermal anomaly detection method is its potential to miss smaller or understory burns. Additionally, prescribed burns, which are typically of low intensity, pose further challenges for satellite detection. Factors such as cloud cover and the timing mismatch between peak burn periods and satellite overpasses further reduce the probability of detection (Nowell et

al., 2018). Consequently, relying solely on thermal anomaly detection may not fully capture all fire events, particularly prescribed burn (Larkin et al., 2020). Moreover, the clustering algorithm employed in this study occasionally misclassifies wildfires as prescribed burn, particularly when their duration is shorter than one day (Li et al., 2023).

The relationship between prescribed burn emissions and corresponding atmospheric pollutants is nonlinear. Therefore, any difference in emissions can lead to significant changes in exposure and associated premature deaths (Clappier et al., 2017). For instance, Koplitz et al. (2018) observed that the Global Burn Emissions Database Version 4.1 (GFEDv4) estimates of burned area for June 2011 were 40% higher than those from FINN over CONUS; however, total organic carbon (OC) emitted by wildfires was two times higher in FINN (0.32 Tg) compared to GFEDv4 (0.15 Tg OC). Also, FINN and GFEDv4 do not exhibit similar seasonal patterns (Larkin et al., 2020). Additionally, Zhang et al. (2014) found that, depending on the inventory used, PM<sub>2.5</sub> emissions from wildland fires in the same region (northern sub-Saharan Africa in this case) could differ by factors of 2–4 annually, and by 8–12 for a specific burn event. However, our estimated total prescribed burn emission of PM<sub>2.5</sub> in 2020 (358 thousand tons) closely aligned with what was reported (334 thousand tons) by the National Emissions Inventory (NEI) for the same year (USEPA, 2023b).

There is significant uncertainty in emissions inventories; examining pollution concentrations from different prescribed burn emission inventories can help to understand the bounds of that uncertainty. Increasing model grid-resolution may also improve performance and should be explored in future studies (Li et al., 2022). The non-CTM-based fusion models to estimate smoke PM<sub>2.5</sub> levels have been reported and they agreed better with observation than CTM, however they are not able to capture the detailed spatial gradients of the smoke PM<sub>2.5</sub> (Childs et al., 2022; Zhang et al., 2023). The lack of near-burn observations to be included in model training can also be attributed to the underestimation of peak smoke PM<sub>2.5</sub> concentrations in these studies where CTMs predicted lower domain-wide average concentrations than the non-CTM models (Kelly et al., 2021). Qiu et al. (2024) observed that in the western US, CTMs overestimate PM<sub>2.5</sub> concentrations during extreme wildfire smoke episodes in 2020 by up to 3-5-fold, while machine learning (ML) estimates are largely consistent with surface measurements. However, in the eastern US, where smoke levels were much lower in 2020, CTMs show modestly better agreement with surface measurements.

The mortality outcomes related to prescribed burn smoke exposure in this study differ from previous research due to varying choices in the selection of CRFs. We used CRFs from GEMM (Burnett et al., 2018) and IER model (Burnett et al., 2014), which commonly hypothesize that PM<sub>2.5</sub> components are equally toxic, regardless of their source. Existing literature is mixed on whether exposure to wildland fire smoke has different health impacts than exposure to air pollution from other sources, as wildland fire PM<sub>2.5</sub> has different composition, and exposure patterns (such as episodic versus consistent exposure) from other sources (Black et al., 2017; DeFlorio-Barker et al., 2019). Some studies found that wildland fire smoke might be more toxic as compared to emissions from other sources like industries and power generation. For instance, Aguilera et al. (2021) reported that exposure to wildfire smoke could lead to a tenfold increase in the risk of respiratory hospitalizations, relative to other PM<sub>2.5</sub> sources that may lie, in part, with the high content of black carbon (BC) and OC and high aromaticity of wildfire PM<sub>2.5</sub>. Similarly, Wei et al.

(2023) observed an annual increase in BC-to-PM<sub>2.5</sub> mass ratio across the US, largely due to rising wildland fire emissions, hinting at potentially higher PM<sub>2.5</sub> toxicity. Past studies have often relied on non-source-specific concentration-response-coefficients (CR-coefficients) for wildland fire PM<sub>2.5</sub>-attributed premature deaths estimations, due to the scarcity of epidemiological studies on PM<sub>2.5</sub> from prescribed burn and associated deaths (Carter et al., 2023; Ford et al., 2018; Pan et al., 2023; Wei et al., 2023). The relative risk estimates from Krewski et al. (2009) have been extensively used for estimating excess long-term all-cause mortality due to wildland fire PM<sub>2.5</sub>. Using the study, we estimated a total of 10,908 deaths (95% CI: 7,347–14,397) during 2013–2020 in ten southeastern states, aligning with IER and GEMM-5COD model results. Ma et al. (2023) found an association between long-term wildfire PM<sub>2.5</sub> exposure and all-cause mortality, with a 0.14% increase in mortality per 1 µg/m<sup>3</sup> rise of wildfire PM<sub>2.5</sub>. Applying this association to prescribed burn, we estimated 2,623 all-cause deaths (95% CI: 2,061–3,184) during the study period, which is much lower than any other selected model in this study.

Previous studies have primarily investigated short-term premature mortality linked to PM<sub>2.5</sub> exposure from prescribed burns. For instance, during a 15-day study period in 2012, in Northern California, short-term exposure to 0.26 µg/m<sup>3</sup> of prescribed burns PM<sub>2.5</sub> was estimated to cause 15 premature deaths (~6 deaths per million acres of burn) (Kiely et al., 2024). Maji et al. (2024) reported 444 premature per year (~200 deaths per million acres of burn) attributed to short-term prescribed burn PM<sub>2.5</sub> exposure to 0.94 µg/m<sup>3</sup> across the Georgia and Surrounding Areas (US) during 2015–2020. The current uncertainty in the impacts of PM<sub>2.5</sub> and MDA8-O<sub>3</sub> from prescribed burn on premature deaths poses a significant challenge in health risk analysis. This underscores the need for further studies on the health effects and toxicity of prescribed burn's pollution versus other sources of pollution. Future research should aim to develop a CR-coefficient specific to prescribed burn PM<sub>2.5</sub> to improve the accuracy of health impact assessments.

Wildfire smoke can travel long distances, carrying O<sub>3</sub> precursors that can be advected into marine environments (Schneider et al., 2024). Studies indicate that O<sub>3</sub> formation from wildfire smoke can increase rapidly over oceanic or estuarine waters due to inhibited deposition, shallower boundary layers, and emissions from ships (Pan and Faloona, 2022). Our findings reflect similar behavior of O<sub>3</sub> over the coastal regions of Georgia, South Carolina, and North Carolina, where prescribed burn can elevate O<sub>3</sub> levels up to ~24 ppb. Likewise, prescribed burn contributed to an increase of ~18 ppb in O<sub>3</sub> levels along the Chesapeake Bay shoreline (Figure S17).

As prescribed burn smoke exposure is anticipated to increase in the future (Swain et al., 2023), and due to growing concern of public health associated with wildfire smoke exposures, there is growing interest to reduce the health-related damages from wildfire events (Cromar et al., 2024; Jonko et al., 2024). The goals of the current actions are to re-introduce smaller and more frequent fires (via prescribed burning) to help reduce the occurrence of large and high-intensity fires (Lydersen et al., 2017; Prichard et al., 2020b). Multiple studies have acknowledged the benefits of fuel reduction via prescribed burning in mitigating wildfire risk but have also highlighted the dangers of introducing additional treatment-related smoke (Jones et al., 2022; Tubbesing et al., 2019). Such studies have called for increased quantification of air-quality and health trade-offs in forest and fire management decision-making (Schollaert et al., 2023).

Wu et al. (2023) found that, the areas in conifer forests in California, US, that have recently burned at low intensity are 64.0% less likely to burn at high intensity in the following years relative to unburned areas. Schollaert et al. (2023) reported that treating 4% of the landscape annually (~3.4% thinning and 0.6% prescribed burns) in the ~1 million ha Tahoe–Central Sierra Initiative area in California could reduce total PM<sub>2.5</sub> smoke concentration by approximately 60% compared to a business-as-usual scenario over a 40-year period. Simulating a 11,220 km<sup>2</sup> wildfire burn area in Northern California under prescribed fire conditions. Kiely et al. (2024) reported a 52% reduction in PM<sub>2.5</sub> emissions, decreasing from 0.27 to 0.14 Tg. Similar findings have been noted in previous studies, where prescribed fires were shown to reduce future wildfire intensity and frequency, thereby decreasing wildfire emissions, as wildfires emit significantly higher amounts of PM<sub>2.5</sub>, with average emission factors ranging from 3 to 20 times greater than those of prescribed fires (Kiely et al., 2024; Kramer et al., 2023; Rosenberg et al., 2024; Williamson et al., 2016). However, the 2019–2020 catastrophic Black Summer wildfires in eastern Australia raised questions about the effectiveness of prescribed burning in mitigating risk under unprecedented fire conditions (Clarke et al., 2022).

Despite some uncertainties, our data links prescribed burn to air quality (Figure S18 and S19) and reveals that exposure to prescribed burn smoke increases burden of premature mortality. These findings highlight the need for targeted public health advisories and emergency response strategies in the southeastern US during high burning days. This study underscores the need for improved air quality management strategies and stronger environmental health policies that consider prescribed burn impacts in urban and rural planning.

#### 4. Conclusion

This comprehensive study quantified the eight year-round impacts of prescribed burn on 24-hour average PM<sub>2.5</sub> and maximum daily 8-hour averaged ozone (MDA8-O<sub>3</sub>) concentrations, as well as associated excess premature mortality due to long-term prescribed burn PM<sub>2.5</sub> and MDA8-O<sub>3</sub> exposure in ten southeastern US states. Prescribed burn emissions were responsible for 15% of the state-level annual average ambient PM<sub>2.5</sub> in Alabama, Florida, Georgia, Mississippi, and South Carolina while their contribution to O<sub>3</sub> was less than 1%. The study also mapped the spatial distributions of prescribed burn-related PM<sub>2.5</sub> and O<sub>3</sub> levels across different seasons, revealing that January–April is the most extensive burning season, significantly affecting air quality. Additionally, it was found that moderate burning season in October–December also significantly impacts air quality, a situation previously unreported. Depending on the concentration response function used, annual premature deaths due to prescribed burn PM<sub>2.5</sub> ranged from 1,076 (IER model) to 2,552 (GEMM-NCD+LRI model) across the ten southeastern states. Furthermore, prescribed burn MDA8-O<sub>3</sub> is responsible for approximately 167 premature deaths annually. Despite a decrease in smoke concentrations in 2020 compared to 2013, premature deaths increased due to an aging population and higher baseline mortality. High premature death rates were especially prominent in urban areas. Given the lack of long-term epidemiological studies specifically on the association between prescribed burn PM<sub>2.5</sub> and premature deaths, this study assumed equivalent responses between prescribed burn PM<sub>2.5</sub> and all-source PM<sub>2.5</sub> in its analysis of premature deaths. If prescribed burn PM<sub>2.5</sub> is more toxic than all-source PM<sub>2.5</sub> as some studies suggest, then associated premature deaths would be higher than estimates in this study. Therefore, conducting more long-term epidemiological studies on the health effects of prescribed burn PM<sub>2.5</sub>

is crucial. Additionally, local policies and guidance are vital to minimize the health risks associated with prescribed burn and protect the public from the adverse effects of exposure to prescribed burn smoke.

## Funding Sources

Research described in this article was conducted under Research Agreement No. 4988-RFA20-1A/21-11 between Georgia Institute of Technology and the Health Effects Institute (HEI), an organization jointly funded by the United States Environmental Protection Agency (EPA) (Assistance Award No. CR-83998101) and certain motor vehicle and engine manufacturers. The contents of this article do not necessarily reflect the views of HEI, or its sponsors, nor do they necessarily reflect the views and policies of the EPA or motor vehicle and engine manufacturers. In addition, KJM and MTO were supported in part by the Centers for Disease Control and Prevention (CDC) under contract number 75D30121P10715 to Georgia Institute of Technology. The views expressed in this article are those of the authors and do not necessarily reflect the views or policies of the CDC.

## Notes

The authors declare no competing financial interest.

## ACKNOWLEDGMENT

This research was supported in part through research cyberinfrastructure resources and services provided by the Partnership for an Advanced Computing Environment (PACE) at the Georgia Institute of Technology, Atlanta, Georgia, USA. All the data are freely available on:  
<https://zenodo.org/records/13380570>

## Appendices

Table A.1. Annual average prescribed burn smoke PM<sub>2.5</sub> in southeastern US states.

States	Prescribed burn smoke PM <sub>2.5</sub> [mean ± SD (median)] (µg/m <sup>3</sup> )									
	2013–2020	2013	2014	2015	2016	2017	2018	2019	2020	
Alabama	0.90±0.15 (0.91)	0.86±0.13 (0.87)	0.80±0.16 (0.81)	1.05±0.21 (1.07)	0.89±0.13 (0.90)	1.09±0.25 (1.04)	0.88±0.19 (0.86)	0.89±0.14 (0.88)	0.82±0.14 (0.82)	
Florida	0.65±0.19 (0.64)	0.75±0.19 (0.77)	0.71±0.12 (0.69)	0.70±0.27 (0.66)	0.65±0.18 (0.65)	0.68±0.28 (0.66)	0.64±0.20 (0.62)	0.54±0.21 (0.51)	0.52±0.23 (0.47)	
Georgia	0.91±0.19 (0.91)	0.80±0.18 (0.79)	0.91±0.18 (0.91)	1.00±0.25 (0.99)	0.94±0.16 (0.96)	1.23±0.32 (1.27)	0.91±0.20 (0.92)	0.80±0.18 (0.83)	0.74±0.2 (0.74)	
Kentucky	0.44±0.05 (0.44)	0.41±0.05 (0.41)	0.33±0.04 (0.33)	0.47±0.06 (0.48)	0.53±0.09 (0.52)	0.56±0.07 (0.56)	0.43±0.06 (0.42)	0.48±0.09 (0.48)	0.38±0.04 (0.38)	
Mississippi	0.65±0.1 (0.64)	0.66±0.08 (0.66)	0.58±0.09 (0.58)	0.74±0.13 (0.73)	0.61±0.12 (0.62)	0.73±0.14 (0.74)	0.58±0.12 (0.58)	0.66±0.12 (0.67)	0.63±0.12 (0.62)	

North Carolina	0.48±0.12 (0.48)	0.35±0.08 (0.35)	0.44±0.1 (0.43)	0.50±0.12 (0.50)	0.60±0.17 (0.59)	0.67±0.19 (0.68)	0.46±0.14 (0.47)	0.49±0.15 (0.50)	0.38±0.09 (0.38)
South Carolina	0.65±0.09 (0.65)	0.54±0.10 (0.52)	0.67±0.09 (0.65)	0.67±0.12 (0.68)	0.72±0.12 (0.72)	0.98±0.14 (1.01)	0.65±0.08 (0.65)	0.58±0.13 (0.57)	0.43±0.06 (0.44)
Tennessee	0.55±0.09 (0.54)	0.52±0.07 (0.52)	0.44±0.06 (0.43)	0.58±0.09 (0.58)	0.63±0.14 (0.63)	0.65±0.1 (0.66)	0.53±0.12 (0.53)	0.61±0.12 (0.62)	0.48±0.08 (0.48)
Virginia	0.37±0.07 (0.38)	0.26±0.04 (0.26)	0.29±0.07 (0.29)	0.38±0.08 (0.38)	0.51±0.10 (0.52)	0.47±0.09 (0.47)	0.38±0.08 (0.38)	0.43±0.09 (0.44)	0.32±0.05 (0.31)
West Virginia	0.33±0.05 (0.33)	0.27±0.04 (0.27)	0.26±0.05 (0.26)	0.31±0.05 (0.31)	0.43±0.07 (0.42)	0.40±0.07 (0.39)	0.33±0.05 (0.34)	0.39±0.07 (0.39)	0.25±0.04 (0.25)

Table A.2. Annual average prescribed burn smoke MDA8-O<sub>3</sub> in southeastern US states.

Prescribed burn smoke MDA8-O <sub>3</sub> [mean ± SD (median)] (ppb)
--

States	2013–2020	2013	2014	2015	2016	2017	2018	2019	2020
Alabama	0.42±0.09 (0.40)	0.54±0.11 (0.51)	0.52±0.13 (0.49)	0.37±0.10 (0.36)	0.34±0.07 (0.33)	0.47±0.15 (0.43)	0.36±0.1 (0.34)	0.38±0.09 (0.37)	0.31±0.08 (0.29)
Florida	0.46±0.12 (0.44)	0.66±0.17 (0.64)	0.63±0.12 (0.63)	0.41±0.12 (0.4)	0.36±0.09 (0.34)	0.44±0.19 (0.41)	0.41±0.15 (0.4)	0.33±0.12 (0.32)	0.35±0.12 (0.34)
Georgia	0.51±0.13 (0.51)	0.61±0.17 (0.59)	0.69±0.16 (0.7)	0.45±0.12 (0.45)	0.44±0.10 (0.44)	0.64±0.19 (0.65)	0.44±0.13 (0.44)	0.42±0.1 (0.41)	0.35±0.12 (0.32)
Kentucky	0.21±0.03 (0.21)	0.27±0.02 (0.27)	0.25±0.04 (0.25)	0.19±0.03 (0.19)	0.18±0.04 (0.18)	0.25±0.04 (0.26)	0.17±0.03 (0.17)	0.22±0.04 (0.23)	0.16±0.02 (0.16)
Mississippi	0.30±0.04 (0.31)	0.41±0.05 (0.41)	0.4±0.07 (0.4)	0.27±0.06 (0.27)	0.23±0.05 (0.24)	0.31±0.07 (0.31)	0.23±0.05 (0.23)	0.27±0.05 (0.27)	0.23±0.04 (0.23)
North Carolina	0.26±0.05 (0.26)	0.25±0.06 (0.25)	0.36±0.08 (0.36)	0.24±0.06 (0.23)	0.25±0.06 (0.24)	0.37±0.09 (0.37)	0.18±0.04 (0.18)	0.25±0.07 (0.25)	0.16±0.04 (0.16)
South Carolina	0.36±0.05 (0.35)	0.39±0.1 (0.37)	0.53±0.07 (0.53)	0.31±0.04 (0.3)	0.32±0.06 (0.31)	0.54±0.08 (0.54)	0.27±0.05 (0.26)	0.29±0.05 (0.29)	0.19±0.03 (0.18)

Tennessee	$0.26 \pm 0.04$ (0.26)	$0.33 \pm 0.04$ (0.33)	$0.31 \pm 0.07$ (0.31)	$0.23 \pm 0.05$ (0.23)	$0.22 \pm 0.07$ (0.22)	$0.29 \pm 0.05$ (0.29)	$0.2 \pm 0.03$ (0.2)	$0.26 \pm 0.06$ (0.26)	$0.18 \pm 0.04$ (0.18)
Virginia	$0.19 \pm 0.04$ (0.19)	$0.20 \pm 0.04$ (0.19)	$0.25 \pm 0.06$ (0.23)	$0.18 \pm 0.04$ (0.18)	$0.21 \pm 0.05$ (0.20)	$0.24 \pm 0.06$ (0.23)	$0.15 \pm 0.03$ (0.14)	$0.22 \pm 0.05$ (0.22)	$0.13 \pm 0.02$ (0.13)
West Virginia	$0.17 \pm 0.02$ (0.18)	$0.21 \pm 0.03$ (0.21)	$0.25 \pm 0.04$ (0.24)	$0.16 \pm 0.02$ (0.16)	$0.17 \pm 0.03$ (0.17)	$0.19 \pm 0.03$ (0.19)	$0.13 \pm 0.02$ (0.13)	$0.20 \pm 0.04$ (0.20)	$0.12 \pm 0.02$ (0.12)

Table A.3. Yearly non-accidental premature deaths attributed to prescribed burn PM<sub>2.5</sub> exposure.

State	GEMM NCD+LRI [mean (95%CI)]							
	2013	2014	2015	2016	2017	2018	2019	2020
Alabama	184 (151-217)	167 (137-197)	325 (264-385)	319 (259-379)	405 (328-481)	50 (41-59)	339 (275-402)	364 (295-433)
Florida	207 (168-244)	215 (176-254)	283 (229-336)	315 (255-375)	328 (265-390)	344 (278-410)	267 (217-318)	295 (239-352)
Georgia	383 (312-451)	430 (351-507)	619 (503-732)	636 (517-754)	839 (681-995)	440 (357-523)	670 (544-794)	665 (539-790)
Kentucky	88 (72-104)	71 (59-84)	118 (97-140)	143 (117-169)	166 (135-197)	732 (593-868)	136 (111-161)	126 (103-150)
Mississippi	68 (55-80)	61 (50-72)	111 (91-133)	101 (82-120)	130 (106-156)	350 (284-416)	112 (91-133)	125 (101-149)

North Carolina	215 (175-254)	271 (221-321)	369 (300-437)	488 (396-578)	563 (457-667)	265 (215-315)	453 (368-537)	428 (347-508)
South Carolina	139 (113-165)	171 (140-203)	214 (174-254)	247 (201-293)	342 (278-406)	243 (197-288)	231 (188-275)	213 (173-254)
Tennessee	152 (124-180)	135 (110-159)	221 (180-261)	263 (214-312)	291 (237-346)	129 (105-152)	279 (227-331)	260 (211-309)
Virginia	116 (94-137)	123 (101-146)	190 (155-226)	274 (223-325)	273 (222-324)	103 (84-123)	251 (204-297)	228 (185-271)
West Virginia	31 (25-37)	29 (24-35)	41 (33-48)	56 (46-67)	58 (48-69)	235 (191-279)	53 (43-63)	43 (36-52)
Total	1583 (128 9- 1869 )	1673 (136 5- 1972 )	2491 (2022- 2948)	2842 (2305- 3366)	3397 (2754- 4026)	2890 (2342- 3428)	2792 (2264- 3307)	2747 (2223- 3262)

Table A.4. Yearly long-term all-cause premature deaths attributed to prescribed burn MDA8-O<sub>3</sub> exposure.

States	all-cause premature deaths [Mean (95% CI)]							
	2013	2014	2015	2016	2017	2018	2019	2020
Alabama	21 (14-28)	19 (13-26)	15 (10-21)	15 (10-20)	20 (13-27)	16 (11-22)	18 (12-24)	14 (9-19)
Florida	29 (19-40)	34 (22-46)	21 (14-29)	18 (12-25)	20 (13-28)	21 (14-29)	17 (12-24)	18 (12-25)
Georgia	43 (28-58)	51 (34-70)	36 (23-49)	39 (26-54)	56 (36-76)	38 (25-52)	41 (27-55)	31 (20-42)

Kentucky	10 (7-14)	9 (7-13)	8 (5-11)	7 (5-10)	11 (7-15)	7 (5-11)	10 (7-14)	7 (5-10)
Mississippi	7 (5-10)	7 (5-10)	5 (3-7)	4 (3-6)	5 (4-8)	4 (3-6)	5 (4-7)	4 (3-6)
North Carolina	21 (14-29)	33 (22-45)	23 (15-32)	26 (17-36)	38 (25-52)	20 (13-27)	30 (20-40)	19 (13-27)
South Carolina	14 (10-20)	21 (14-29)	13 (9-18)	13 (9-19)	23 (15-32)	12 (8-17)	14 (10-20)	9 (6-13)
Tennessee	16 (11-23)	16 (11-22)	13 (9-18)	13 (9-17)	16 (11-22)	11 (8-16)	16 (11-22)	11 (8-16)
Virginia	12 (8-17)	15 (10-21)	12 (8-17)	14 (10-20)	17 (11-24)	10 (7-14)	15 (10-21)	11 (7-15)
West Virginia	3 (3-5)	4 (3-6)	3 (2-4)	3 (2-4)	3 (3-5)	2 (2-3)	3 (3-5)	2 (2-3)
Total	177 (115-240)	209 (135-283)	146 (95-198)	153 (99-207)	209 (135-284)	143 (92-194)	169 (109-229)	127 (82-172)



## References

- Afrin, S., Garcia-Menendez, F., 2020. The Influence of Prescribed Fire on Fine Particulate Matter Pollution in the Southeastern United States. *Geophys Res Lett* 47. <https://doi.org/10.1029/2020GL088988>
- Aguilera, R., Corrington, T., Gershunov, A., Benmarhnia, T., 2021. Wildfire smoke impacts respiratory health more than fine particles from other sources: observational evidence from Southern California. *Nat Commun* 12, 1493. <https://doi.org/10.1038/s41467-021-21708-0>
- Anenberg, S.C., Horowitz, L.W., Tong, D.Q., West, J.J., 2010. An Estimate of the Global Burden of Anthropogenic Ozone and Fine Particulate Matter on Premature Human Mortality Using Atmospheric Modeling. *Environ Health Perspect* 118, 1189–1195. <https://doi.org/10.1289/ehp.0901220>
- Appel, K.W., Bash, J.O., Fahey, K.M., Foley, K.M., Gilliam, R.C., Hogrefe, C., Hutzell, W.T., Kang, D., Mathur, R., Murphy, B.N., Napelenok, S.L., Nolte, C.G., Pleim, J.E., Pouliot, G.A., Pye, H.O.T., Ran, L., Roselle, S.J., Sarwar, G., Schwede, D.B., Sidi, F.I., Spero, T.L., Wong, D.C., 2021. The Community Multiscale Air Quality (CMAQ) model versions 5.3 and 5.3.1: system updates and evaluation. *Geosci Model Dev* 14, 2867–2897. <https://doi.org/10.5194/gmd-14-2867-2021>
- Baijnath-Rodino, J.A., Li, S., Martinez, A., Kumar, M., Quinn-Davidson, L.N., York, R.A., Banerjee, T., 2022. Historical seasonal changes in prescribed burn windows in California. *Science of The Total Environment* 836, 155723. <https://doi.org/10.1016/j.scitotenv.2022.155723>
- Black, C., Tesfaigzi, Y., Bassein, J.A., Miller, L.A., 2017. Wildfire smoke exposure and human health: Significant gaps in research for a growing public health issue. *Environ Toxicol Pharmacol* 55, 186–195. <https://doi.org/10.1016/j.etap.2017.08.022>
- Boby, L.A., Fawcett, J.E., Clabo, D., Harriman, H., Maggard, A., Coulliette, B., Kays, L. & McNair, S. (2023). Guidebook for Prescribed Burning in the Southern Region. University of Georgia Cooperative Extension Bulletin 1560. UGA Warnell School of Forestry & Natural Resources Outreach Publication, WSFNR-23-16A.
- Burke, M., Childs, M.L., de la Cuesta, B., Qiu, M., Li, J., Gould, C.F., Heft-Neal, S., Wara, M., 2023. The contribution of wildfire to PM<sub>2.5</sub> trends in the USA. *Nature* 622, 761–766. <https://doi.org/10.1038/s41586-023-06522-6>
- Burke, M., Driscoll, A., Heft-Neal, S., Xue, J., Burney, J., Wara, M., 2021. The changing risk and burden of wildfire in the United States. *Proceedings of the National Academy of Sciences* 118. <https://doi.org/10.1073/pnas.2011048118>
- Burnett, R., Chen, H., Szyszkowicz, M., Fann, N., Hubbell, B., Pope, C.A., Apte, J.S., Brauer, M., Cohen, A., Weichenthal, S., Coggins, J., Di, Q., Brunekreef, B., Frostad, J., Lim, S.S., Kan,

- H., Walker, K.D., Thurston, G.D., Hayes, R.B., Lim, C.C., Turner, M.C., Jerrett, M., Krewski, D., Gapstur, S.M., Diver, W.R., Ostro, B., Goldberg, D., Crouse, D.L., Martin, R. V., Peters, P., Pinault, L., Tjepkema, M., van Donkelaar, A., Villeneuve, P.J., Miller, A.B., Yin, P., Zhou, M., Wang, L., Janssen, N.A.H., Marra, M., Atkinson, R.W., Tsang, H., Quoc Thach, T., Cannon, J.B., Allen, R.T., Hart, J.E., Laden, F., Cesaroni, G., Forastiere, F., Weinmayr, G., Jaensch, A., Nagel, G., Concin, H., Spadaro, J. V., 2018. Global estimates of mortality associated with long-term exposure to outdoor fine particulate matter. *Proceedings of the National Academy of Sciences* 115, 9592–9597. <https://doi.org/10.1073/pnas.1803222115>
- Burnett, R.T., Pope, C.A., Ezzati, M., Olives, C., Lim, S.S., Mehta, S., Shin, H.H., Singh, G., Hubbell, B., Brauer, M., Anderson, H.R., Smith, K.R., Balmes, J.R., Bruce, N.G., Kan, H., Laden, F., Prüss-Ustün, A., Turner, M.C., Gapstur, S.M., Diver, W.R., Cohen, A., 2014. An Integrated Risk Function for Estimating the Global Burden of Disease Attributable to Ambient Fine Particulate Matter Exposure. *Environ Health Perspect* 122, 397–403. <https://doi.org/10.1289/ehp.1307049>
- Carter, T.S., Heald, C.L., Selin, N.E., 2023. Large mitigation potential of smoke PM<sub>2.5</sub> in the US from human-ignited fires. *Environmental Research Letters* 18, 014002. <https://doi.org/10.1088/1748-9326/aca91f>
- Childs, M.L., Li, J., Wen, J., Heft-Neal, S., Driscoll, A., Wang, S., Gould, C.F., Qiu, M., Burney, J., Burke, M., 2022. Daily Local-Level Estimates of Ambient Wildfire Smoke PM<sub>2.5</sub> for the Contiguous US. *Environ Sci Technol* 56, 13607–13621. <https://doi.org/10.1021/acs.est.2c02934>
- Clappier, A., Belis, C.A., Pernigotti, D., Thunis, P., 2017. Source apportionment and sensitivity analysis: two methodologies with two different purposes. *Geosci Model Dev* 10, 4245–4256. <https://doi.org/10.5194/gmd-10-4245-2017>
- Clarke, H., Cirulis, B., Penman, T., Price, O., Boer, M.M., Bradstock, R., 2022. The 2019–2020 Australian forest fires are a harbinger of decreased prescribed burning effectiveness under rising extreme conditions. *Sci Rep* 12, 11871. <https://doi.org/10.1038/s41598-022-15262-y>
- Cromar, K., Gladson, L., Gohlke, J., Li, Y., Tong, D., Ewart, G., 2024. Adverse Health Impacts of Outdoor Air Pollution, Including from Wildland Fires, in the United States: “Health of the Air,” 2018–2020. *Ann Am Thorac Soc* 21, 76–87. <https://doi.org/10.1513/AnnalsATS.202305-455OC>
- DeFlorio-Barker, S., Crooks, J., Reyes, J., Rappold, A.G., 2019. Cardiopulmonary Effects of Fine Particulate Matter Exposure among Older Adults, during Wildfire and Non-Wildfire Periods, in the United States 2008–2010. *Environ Health Perspect* 127. <https://doi.org/10.1289/EHP3860>
- D’Evelyn, S.M., Jung, J., Alvarado, E., Baumgartner, J., Caligiuri, P., Hagmann, R.K., Henderson, S.B., Hessburg, P.F., Hopkins, S., Kasner, E.J., Krawchuk, M.A., Krenz, J.E., Lydersen, J.M., Marlier, M.E., Masuda, Y.J., Metlen, K., Mittelstaedt, G., Prichard, S.J., Schollaert, C.L., Smith, E.B., Stevens, J.T., Tessum, C.W., Reeb-Whitaker, C., Wilkins, J.L., Wolff, N.H., Wood, L.M., Haugo, R.D., Spector, J.T., 2022. Wildfire, Smoke Exposure, Human Health,

- and Environmental Justice Need to be Integrated into Forest Restoration and Management. *Curr Environ Health Rep* 9, 366–385. <https://doi.org/10.1007/s40572-022-00355-7>
- Emery, C., Liu, Z., Russell, A.G., Odman, M.T., Yarwood, G., Kumar, N., 2017. Recommendations on statistics and benchmarks to assess photochemical model performance. *J Air Waste Manage Assoc* 67, 582–598. <https://doi.org/10.1080/10962247.2016.1265027>
- Ford, B., Val Martin, M., Zelasky, S.E., Fischer, E. V., Anenberg, S.C., Heald, C.L., Pierce, J.R., 2018. Future Fire Impacts on Smoke Concentrations, Visibility, and Health in the Contiguous United States. *Geohealth* 2, 229–247. <https://doi.org/10.1029/2018GH000144>
- Friberg, M.D., Zhai, X., Holmes, H.A., Chang, H.H., Strickland, M.J., Sarnat, S.E., Tolbert, P.E., Russell, A.G., Mulholland, J.A., 2016. Method for Fusing Observational Data and Chemical Transport Model Simulations To Estimate Spatiotemporally Resolved Ambient Air Pollution. *Environ Sci Technol* 50, 3695–3705. <https://doi.org/10.1021/acs.est.5b05134>
- Glassman, S.I., Randolph, J.W.J., Saroa, S.S., Capocchi, J.K., Walters, K.E., Pulido-Chavez, M.F., Larios, L., 2023. Prescribed versus wildfire impacts on exotic plants and soil microbes in California grasslands. *Applied Soil Ecology* 185, 104795. <https://doi.org/10.1016/j.apsoil.2022.104795>
- Hu, Y., Odman, M.T., Russell, A.G., Kumar, N., Knipping, E., 2022. Source apportionment of ozone and fine particulate matter in the United States for 2016 and 2028. *Atmos Environ* 285, 119226. <https://doi.org/10.1016/j.atmosenv.2022.119226>
- Huang, R., Zhang, X., Chan, D., Kondragunta, S., Russell, A.G., Odman, M.T., 2018. Burned Area Comparisons Between Prescribed Burning Permits in Southeastern United States and Two Satellite-Derived Products. *Journal of Geophysical Research: Atmospheres* 123, 4746–4757. <https://doi.org/10.1029/2017JD028217>
- IHME, 2019. GBD Results [WWW Document]. URL <https://vizhub.healthdata.org/gbd-results/> (accessed 2.11.24).
- Jaffe, D.A., O'Neill, S.M., Larkin, N.K., Holder, A.L., Peterson, D.L., Halofsky, J.E., Rappold, A.G., 2020. Wildfire and prescribed burning impacts on air quality in the United States. *J Air Waste Manage Assoc* 70, 583–615. <https://doi.org/10.1080/10962247.2020.1749731>
- Jones, B.A., McDermott, S., Champ, P.A., Berrens, R.P., 2022. More smoke today for less smoke tomorrow? We need to better understand the public health benefits and costs of prescribed fire. *Int J Wildland Fire* 31, 918–926. <https://doi.org/10.1071/WF22025>
- Jonko, A., Oliveto, J., Beaty, T., Atchley, A., Battaglia, M.A., Dickinson, M.B., Gallagher, M.R., Gilbert, A., Godwin, D., Kupfer, J.A., Hiers, J.K., Hoffman, C., North, M., Restaino, J., Sieg, C., Skowronski, N., 2024. How will future climate change impact prescribed fire across the contiguous United States? *NPJ Clim Atmos Sci* 7, 96. <https://doi.org/10.1038/s41612-024-00649-7>

- Kelly, J.T., Jang, C., Timin, B., Di, Q., Schwartz, J., Liu, Y., van Donkelaar, A., Martin, R. V., Berrocal, V., Bell, M.L., 2021. Examining PM<sub>2.5</sub> concentrations and exposure using multiple models. Environ Res 196, 110432. <https://doi.org/10.1016/j.envres.2020.110432>
- Kiely, L., Neyestani, S.E., Binte-Shahid, S., York, R.A., Porter, W.C., Barsanti, K.C., 2024. California Case Study of Wildfires and Prescribed Burns: PM<sub>2.5</sub> Emissions, Concentrations, and Implications for Human Health. Environ Sci Technol 58, 5210–5219. <https://doi.org/10.1021/acs.est.3c06421>
- Kondo, M.C., Reid, C.E., Mockrin, M.H., Heilman, W.E., Long, D., 2022. Socio-demographic and health vulnerability in prescribed-burn exposed versus unexposed counties near the National Forest System. Science of The Total Environment 806, 150564. <https://doi.org/10.1016/j.scitotenv.2021.150564>
- Koplotz, S.N., Nolte, C.G., Pouliot, G.A., Vukovich, J.M., Beidler, J., 2018. Influence of uncertainties in burned area estimates on modeled wildland fire PM<sub>2.5</sub> and ozone pollution in the contiguous U.S. Atmos Environ 191, 328–339. <https://doi.org/10.1016/j.atmosenv.2018.08.020>
- Kramer, S.J., Huang, S., McClure, C.D., Chaveste, M.R., Lurmann, F., 2023. Projected smoke impacts from increased prescribed fire activity in California's high wildfire risk landscape. Atmos Environ 311, 119993. <https://doi.org/10.1016/j.atmosenv.2023.119993>
- Krewski, D., Jerrett, M., Burnett, R.T., Ma, R., Hughes, E., Shi, Y., Turner, M.C., Pope, C.A., Thurston, G., Calle, E.E., Thun, M.J., Beckerman, B., DeLuca, P., Finkelstein, N., Ito, K., Moore, D.K., Newbold, K.B., Ramsay, T., Ross, Z., Shin, H., Tempalski, B., 2009. Extended follow-up and spatial analysis of the American Cancer Society study linking particulate air pollution and mortality. Res Rep Health Eff Inst 5–114; discussion 115-36.
- Larkin, N.K., Raffuse, S.M., Huang, S., Pavlovic, N., Lahm, P., Rao, V., 2020. The Comprehensive Fire Information Reconciled Emissions (CFIRE) inventory: Wildland fire emissions developed for the 2011 and 2014 U.S. National Emissions Inventory. J Air Waste Manage Assoc 70, 1165–1185. <https://doi.org/10.1080/10962247.2020.1802365>
- Li, F., Zhang, X., Kondragunta, S., Schmidt, C.C., Holmes, C.D., 2020. A preliminary evaluation of GOES-16 active fire product using Landsat-8 and VIIRS active fire data, and ground-based prescribed fire records. Remote Sens Environ 237, 111600. <https://doi.org/10.1016/j.rse.2019.111600>
- Li, Y., Kumar, A., Hamilton, S., Lea, J.D., Harvey, J., Kleeman, M.J., 2022. Optimized environmental justice calculations for air pollution disparities in Southern California. Heliyon 8, e10732. <https://doi.org/10.1016/j.heliyon.2022.e10732>
- Liu, Y. (2014). A Regression Model for Smoke Plume Rise of Prescribed Fires Using Meteorological Conditions. Journal of Applied Meteorology and Climatology, 53(8), 1961–1975. <https://doi.org/10.1175/JAMC-D-13-0114.1>

Li, Z., Maji, K.J., Hu, Y., Vaidyanathan, A., O'Neill, S.M., Odman, M.T., Russell, A.G., 2023. An Analysis of Prescribed Fire Activities and Emissions in the Southeastern United States from 2013 to 2020. *Remote Sens (Basel)* 15, 2725. <https://doi.org/10.3390/rs15112725>

Lydersen, J.M., Collins, B.M., Brooks, M.L., Matchett, J.R., Shive, K.L., Povak, N.A., Kane, V.R., Smith, D.F., 2017. Evidence of fuels management and fire weather influencing fire severity in an extreme fire event. *Ecological Applications* 27, 2013–2030. <https://doi.org/10.1002/eap.1586>

Ma, Y., Zang, E., Liu, Y., Lu, Y., Krumholz, H.M., Bell, M.L., Chen, K., 2023. Long-term exposure to wildfire smoke PM<sub>2.5</sub> and mortality in the contiguous United States. *medRxiv*. <https://doi.org/10.1101/2023.01.31.23285059>

Maji, K.J., Li, Z., Vaidyanathan, A., Hu, Y., Stowell, J.D., Milano, C., Wellenius, G., Kinney, P.L., Russell, A.G., Odman, M.T., 2024. Estimated Impacts of Prescribed Fires on Air Quality and Premature Deaths in Georgia and Surrounding Areas in the US, 2015–2020. *Environ Sci Technol*. <https://doi.org/10.1021/acs.est.4c00890>

Maji, K.J., Namdeo, A., Bramwell, L., 2023. Driving factors behind the continuous increase of long-term PM<sub>2.5</sub>-attributable health burden in India using the high-resolution global datasets from 2001 to 2020. *Science of The Total Environment* 866, 161435. <https://doi.org/10.1016/j.scitotenv.2023.161435>

Melvin, M.A., 2018. National prescribed fire use survey report. National Association of State Foresters and the Coalition of Prescribed Fire Councils. Available online at: <https://www.stateforesters.org/wp-content/uploads/2018/12/2018-Prescribed-Fire-Use-Survey-Report-1.pdf>.

Michael, R., Mirabelli, M.C., Vaidyanathan, A., 2023. Public health applications of historical smoke forecasts: An evaluation of archived BlueSky data for the coterminous United States, 2015–2018. *Comput Geosci* 171, 105267. <https://doi.org/10.1016/j.cageo.2022.105267>

Neumann, J.E., Amend, M., Anenberg, S., Kinney, P.L., Sarofim, M., Martinich, J., Lukens, J., Xu, J.-W., Roman, H., 2021. Estimating PM<sub>2.5</sub>-related premature mortality and morbidity associated with future wildfire emissions in the western US. *Environmental Research Letters* 16, 035019. <https://doi.org/10.1088/1748-9326/abe82b>

NOAA, 2020. March 2020 National Climate Report.

Nowell, H.K., Holmes, C.D., Robertson, K., Teske, C., Hiers, J.K., 2018. A New Picture of Fire Extent, Variability, and Drought Interaction in Prescribed Fire Landscapes: Insights From Florida Government Records. *Geophys Res Lett* 45, 7874–7884. <https://doi.org/10.1029/2018GL078679>

O'Dell, K., Ford, B., Fischer, E. V., Pierce, J.R., 2019. Contribution of Wildland-Fire Smoke to US PM<sub>2.5</sub> and Its Influence on Recent Trends. *Environ Sci Technol* 53, 1797–1804. <https://doi.org/10.1021/acs.est.8b05430>

Ottmar, R.D., Sandberg, D. V., Riccardi, C.L., Prichard, S.J., 2007. An overview of the Fuel Characteristic Classification System — Quantifying, classifying, and creating fuelbeds for resource planningThis article is one of a selection of papers published in the Special Forum on the Fuel Characteristic Classification System. Canadian Journal of Forest Research 37, 2383–2393. <https://doi.org/10.1139/X07-077>

Pan, K., Faloona, I.C., 2022. The impacts of wildfires on ozone production and boundary layer dynamics in California's Central Valley. Atmos Chem Phys 22, 9681–9702. <https://doi.org/10.5194/acp-22-9681-2022>

Pan, S., Gan, L., Jung, J., Yu, W., Roy, A., Diao, L., Jeon, W., Souri, A.H., Gao, H.O., Choi, Y., 2023. Quantifying the premature mortality and economic loss from wildfire-induced PM<sub>2.5</sub> in the contiguous U.S. Science of The Total Environment 875, 162614. <https://doi.org/10.1016/j.scitotenv.2023.162614>

Pozzer, A., Anenberg, S.C., Dey, S., Haines, A., Lelieveld, J., Chowdhury, S., 2023. Mortality Attributable to Ambient Air Pollution: A Review of Global Estimates. Geohealth 7. <https://doi.org/10.1029/2022GH000711>

Prichard, S.J., Kennedy, M.C., Wright, C.S., Cronan, J.B., Ottmar, R.D., 2017. Predicting forest floor and woody fuel consumption from prescribed burns in southern and western pine ecosystems of the United States. For Ecol Manage 405, 328–338. <https://doi.org/10.1016/j.foreco.2017.09.025>

Prichard, S.J., O'Neill, S.M., Eagle, P., Andreu, A.G., Drye, B., Dubowy, J., Urbanski, S., Strand, T.M., 2020a. Wildland fire emission factors in North America: synthesis of existing data, measurement needs and management applications. Int J Wildland Fire 29, 132. <https://doi.org/10.1071/WF19066>

Prichard, S.J., Povak, N.A., Kennedy, M.C., Peterson, D.W., 2020b. Fuel treatment effectiveness in the context of landform, vegetation, and large, wind-driven wildfires. Ecological Applications 30. <https://doi.org/10.1002/eap.2104>

Qiu, M., Kelp, M., Heft-Neal, S., Jin, X., Gould, C.F., Tong, D.Q., Burke, M., 2024. Evaluating estimation methods for wildfire smoke and their implications for assessing health effects. <https://doi.org/10.31223/x59m59>

Reid, A.M., Robertson, K.M., Hmielowski, T.L., 2012. Predicting litter and live herb fuel consumption during prescribed fires in native and old-field upland pine communities of the southeastern United States. Canadian Journal of Forest Research 42, 1611–1622. <https://doi.org/10.1139/x2012-096>

Rosenberg, A., Hoshiko, S., Buckman, J.R., Yeomans, K.R., Hayashi, T., Kramer, S.J., Huang, S., French, N.H.F., Rappold, A.G., 2024. Health Impacts of Future Prescribed Fire Smoke: Considerations From an Exposure Scenario in California. Earths Future 12. <https://doi.org/10.1029/2023EF003778>

Schneider, S.R., Shi, B., Abbatt, J.P.D., 2024. The Measured Impact of Wildfires on Ozone in Western Canada From 2001 to 2019. *Journal of Geophysical Research: Atmospheres* 129. <https://doi.org/10.1029/2023JD038866>

Schollaert, C.L., Jung, J., Wilkins, J., Alvarado, E., Baumgartner, J., Brun, J., Busch Isaksen, T., Lydersen, J.M., Marlier, M.E., Marshall, J.D., Masuda, Y.J., Maxwell, C., Tessum, C.W., Wilson, K.N., Wolff, N.H., Spector, J.T., 2023. Quantifying the smoke-related public health trade-offs of forest management. *Nat Sustain.* <https://doi.org/10.1038/s41893-023-01253-y>

Senthilkumar, N., Gilfether, M., Metcalf, F., Russell, A.G., Mulholland, J.A., Chang, H.H., 2019. Application of a Fusion Method for Gas and Particle Air Pollutants between Observational Data and Chemical Transport Model Simulations Over the Contiguous United States for 2005–2014. *Int J Environ Res Public Health* 16, 3314. <https://doi.org/10.3390/ijerph16183314>

Skamarock, W.C., Klemp, J.B., Dudhia, J., Gill, D.O., Barker, D.M., Duda, M.G., Huang, X.Y., Wang, W. and Powers, J.G., 2008. A description of the advanced research WRF version 3. NCAR technical note, 475(125), pp.10-5065.

Sun, H.Z., Yu, P., Lan, C., Wan, M.W.L., Hickman, S., Murulitharan, J., Shen, H., Yuan, L., Guo, Y., Archibald, A.T., 2022. Cohort-based long-term ozone exposure-associated mortality risks with adjusted metrics: A systematic review and meta-analysis. *The Innovation* 3, 100246. <https://doi.org/10.1016/j.xinn.2022.100246>

Swain, D.L., Abatzoglou, J.T., Kolden, C., Shive, K., Kalashnikov, D.A., Singh, D., Smith, E., 2023. Climate change is narrowing and shifting prescribed fire windows in western United States. *Commun Earth Environ* 4, 340. <https://doi.org/10.1038/s43247-023-00993-1>

Tubbesing, C.L., Fry, D.L., Roller, G.B., Collins, B.M., Fedorova, V.A., Stephens, S.L., Battles, J.J., 2019. Strategically placed landscape fuel treatments decrease fire severity and promote recovery in the northern Sierra Nevada. *For Ecol Manage* 436, 45–55. <https://doi.org/10.1016/j.foreco.2019.01.010>

USEPA, 2023a. Wildland Fire, Air Quality, and Public Health Considerations Fact Sheet.

USEPA, 2023b. 2020 National Emissions Inventory (NEI) Data [WWW Document]. URL <https://www.epa.gov/air-emissions-inventories/2020-national-emissions-inventory-nei-data> (accessed 2.11.24).

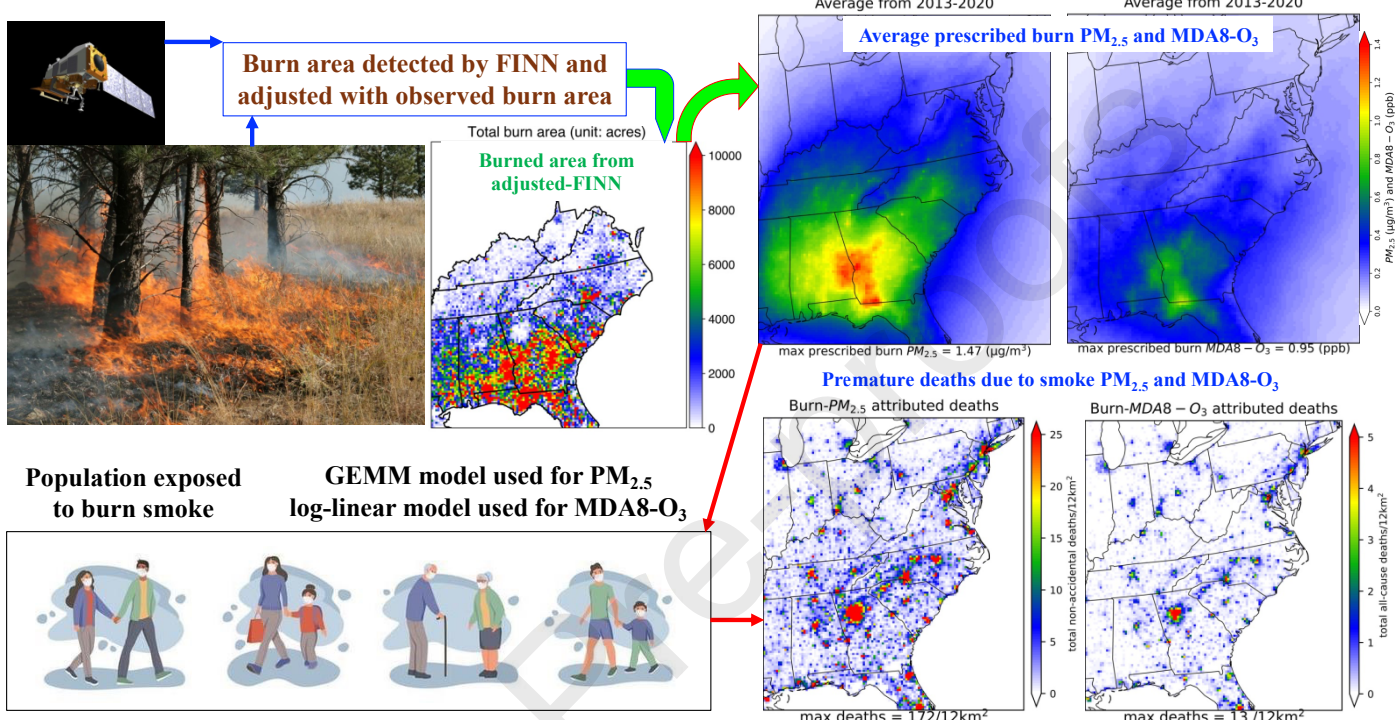
USEPA, 2019. Exceptional Events Guidance: Prescribed Fire on Wildland that May Influence Ozone and Particulate Matter Concentrations . Research Triangle Park, NC .

van Donkelaar, A., Martin, R. V., Brauer, M., Kahn, R., Levy, R., Verduzco, C., Villeneuve, P.J., 2010. Global Estimates of Ambient Fine Particulate Matter Concentrations from Satellite-Based Aerosol Optical Depth: Development and Application. *Environ Health Perspect* 118, 847–855. <https://doi.org/10.1289/ehp.0901623>

- Wei, J., Wang, J., Li, Z., Kondragunta, S., Anenberg, S., Wang, Y., Zhang, H., Diner, D., Hand, J., Lyapustin, A., Kahn, R., Colarco, P., da Silva, A., Ichoku, C., 2023. Long-term mortality burden trends attributed to black carbon and PM<sub>2.5</sub> from wildfire emissions across the continental USA from 2000 to 2020: a deep learning modelling study. *Lancet Planet Health* 7, e963–e975. [https://doi.org/10.1016/S2542-5196\(23\)00235-8](https://doi.org/10.1016/S2542-5196(23)00235-8)
- Wiedinmyer, C., Kimura, Y., McDonald-Buller, E.C., Emmons, L.K., Buchholz, R.R., Tang, W., Seto, K., Joseph, M.B., Barsanti, K.C., Carlton, A.G., Yokelson, R., 2023. The Fire Inventory from NCAR version 2.5: an updated global fire emissions model for climate and chemistry applications. *Geosci Model Dev* 16, 3873–3891. <https://doi.org/10.5194/gmd-16-3873-2023>
- Williamson, G.J., Bowman, D.M.J.S., Price, O.F., Henderson, S.B., Johnston, F.H., 2016. A transdisciplinary approach to understanding the health effects of wildfire and prescribed fire smoke regimes. *Environmental Research Letters* 11, 125009. <https://doi.org/10.1088/1748-9326/11/12/125009>
- WorldPop, 2023. Open Spatial Demographic Data and Research [WWW Document]. URL <https://www.worldpop.org/> (accessed 1.1.24).
- Wright, C.S., 2013. Fuel Consumption Models for Pine Flatwoods Fuel Types in the Southeastern United States. *Southern Journal of Applied Forestry* 37, 148–159. <https://doi.org/10.5849/sjaf.12-006>
- Wu, X., Sverdrup, E., Mastrandrea, M.D., Wara, M.W., Wager, S., 2023. Low-intensity fires mitigate the risk of high-intensity wildfires in California's forests. *Sci Adv* 9. <https://doi.org/10.1126/sciadv.adj4123>
- Xu, R., Ye, T., Yue, X., Yang, Z., Yu, W., Zhang, Yiwen, Bell, M.L., Morawska, L., Yu, P., Zhang, Yuxi, Wu, Y., Liu, Y., Johnston, F., Lei, Y., Abramson, M.J., Guo, Y., Li, S., 2023. Global population exposure to landscape fire air pollution from 2000 to 2019. *Nature* 621, 521–529. <https://doi.org/10.1038/s41586-023-06398-6>
- Zhang, D., Wang, W., Xi, Y., Bi, J., Hang, Y., Zhu, Q., Pu, Q., Chang, H., Liu, Y., 2023. Wildland Fires Worsened Population Exposure to PM<sub>2.5</sub> Pollution in the Contiguous United States. *Environ Sci Technol* 57, 19990–19998. <https://doi.org/10.1021/acs.est.3c05143>
- Zhang, F., Wang, J., Ichoku, C., Hyer, E.J., Yang, Z., Ge, C., Su, S., Zhang, X., Kondragunta, S., Kaiser, J.W., Wiedinmyer, C., da Silva, A., 2014. Sensitivity of mesoscale modeling of smoke direct radiative effect to the emission inventory: a case study in northern sub-Saharan African region. *Environmental Research Letters* 9, 075002. <https://doi.org/10.1088/1748-9326/9/7/075002>

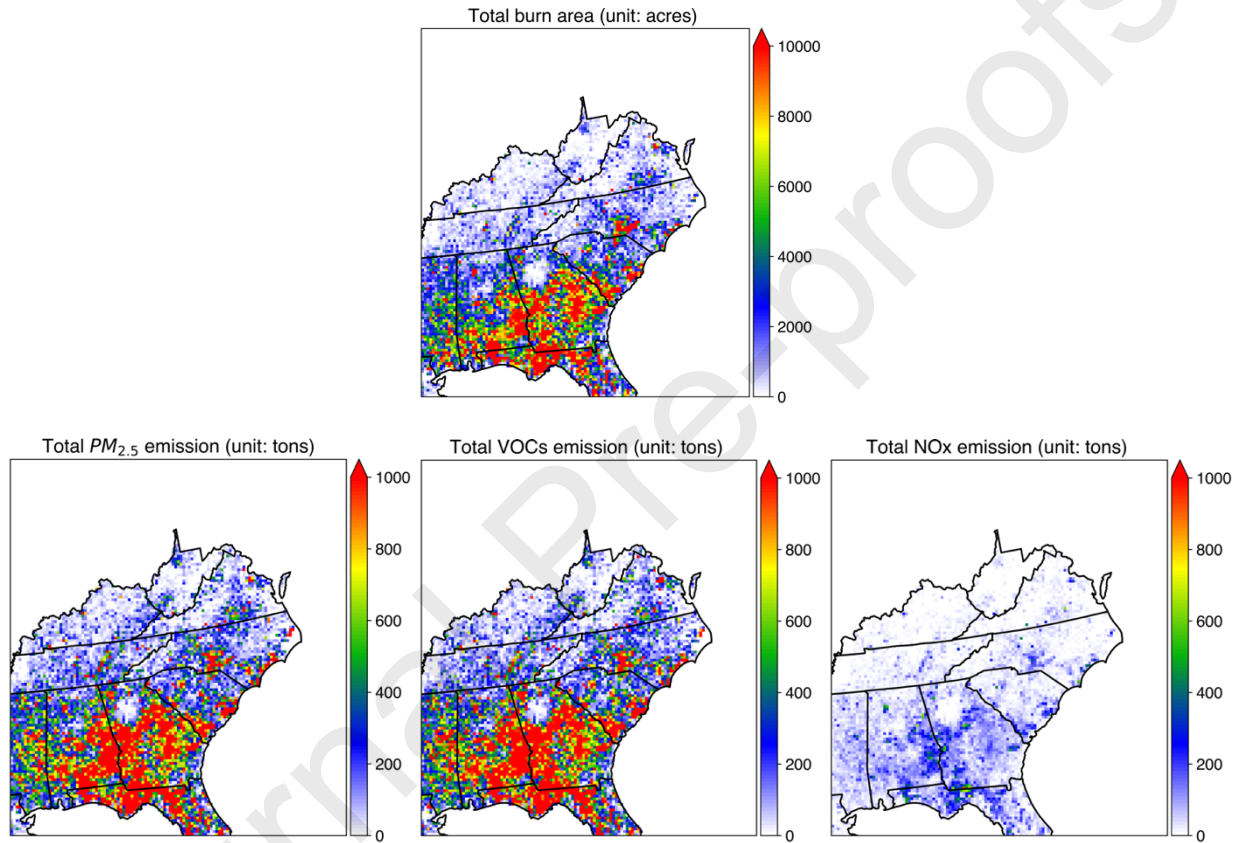
## Graphical Abstract

### Prescribed burn impacts in 10 southeastern US states

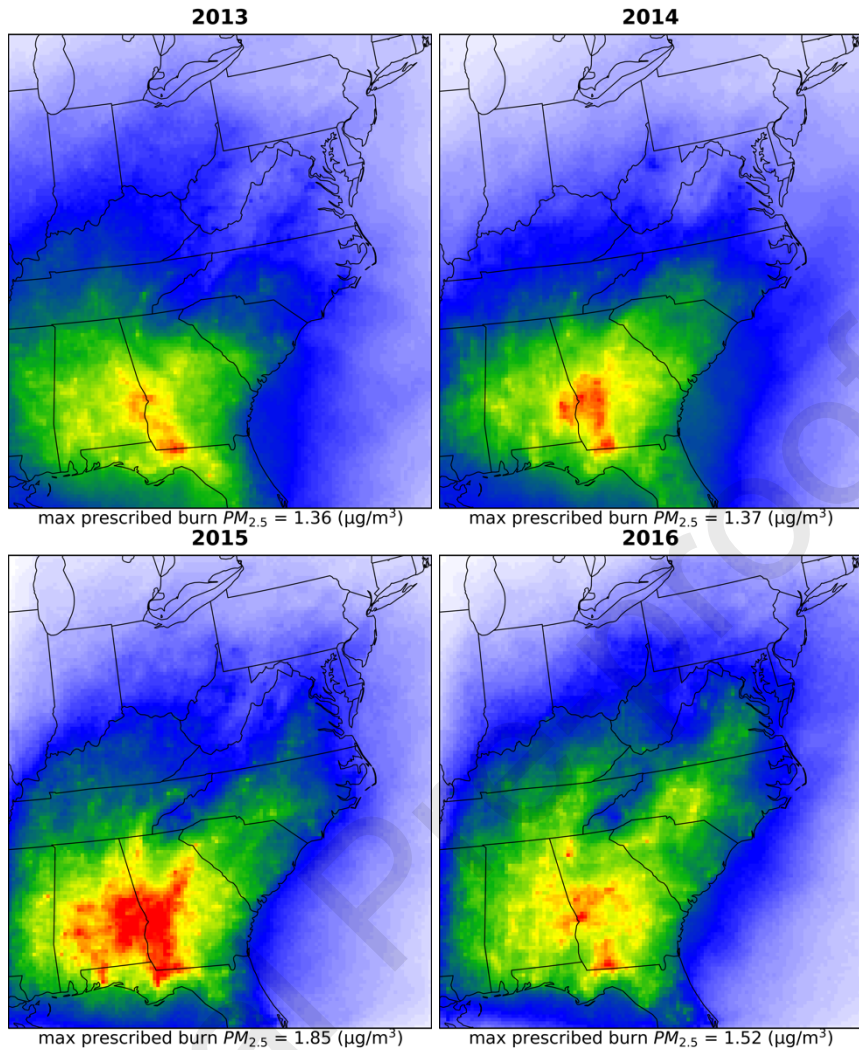


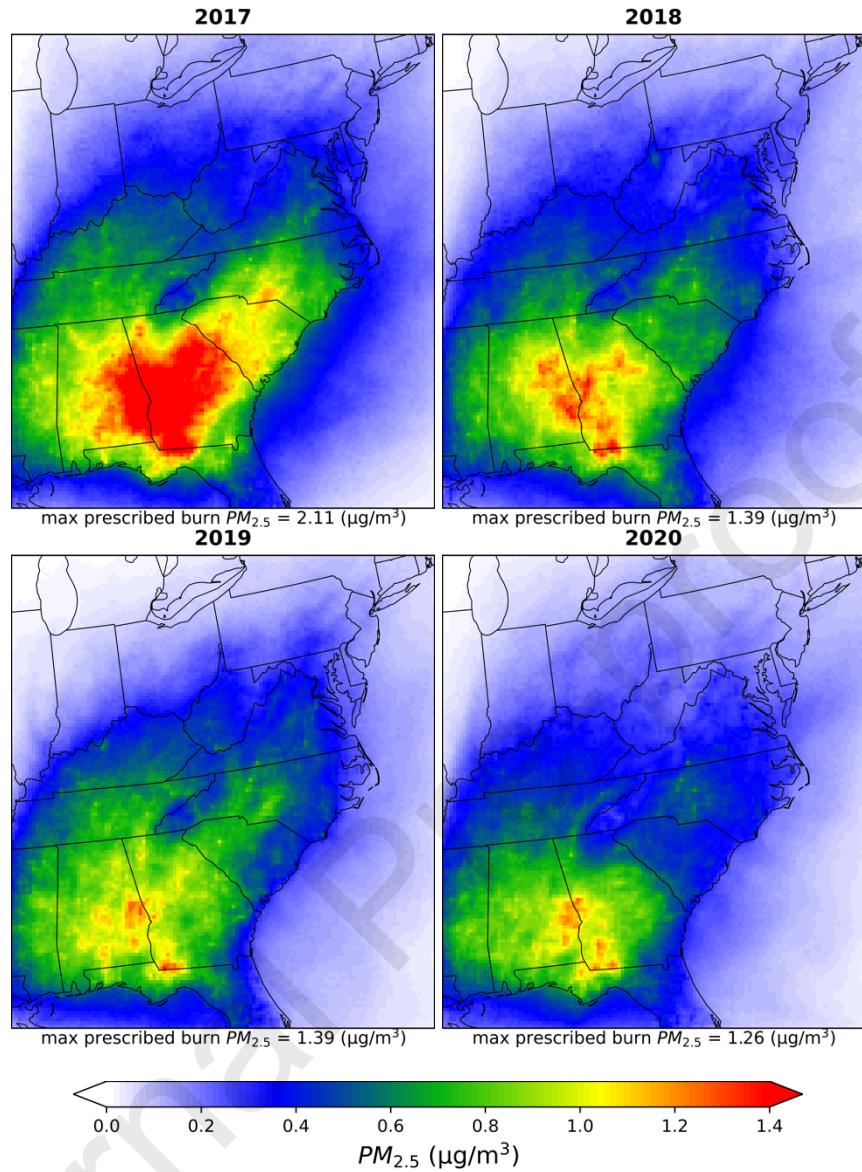
**Highlights:**

- Prescribed burns are a major source of air pollution in the southeastern US.
- A total of 25.1 million acres of land were treated with prescribed burns in the ten southeastern US states during 2013–2020.
- Approximately 15% of ambient PM<sub>2.5</sub> in Alabama, Florida, Georgia, Mississippi, and South Carolina originates from prescribed burns.
- Prescribed burns were responsible for an average 1.0% increase in ambient MDA8-O<sub>3</sub> in Alabama, Florida, Georgia, and South Carolina.
- Prescribed burn PM<sub>2.5</sub> and MDA8-O<sub>3</sub> resulted in a total of 20,416 excess non-accidental and 1,332 all-cause premature deaths in the ten southeastern states.

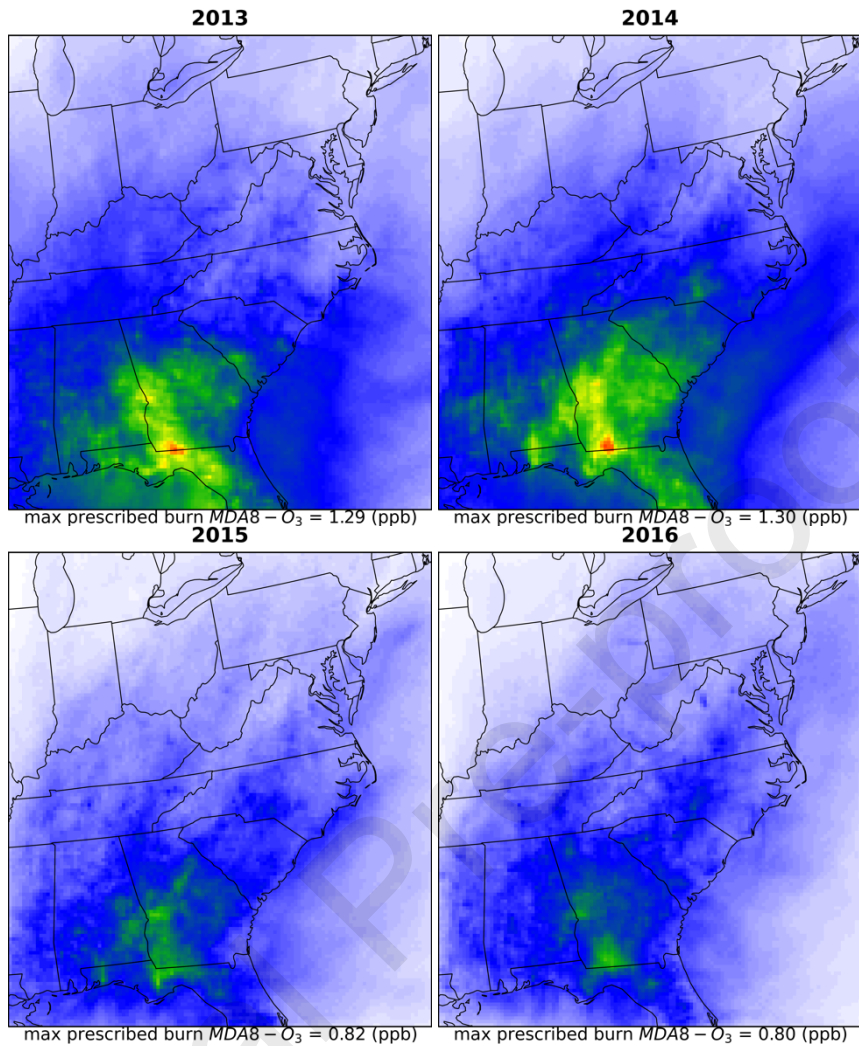
**Figures**

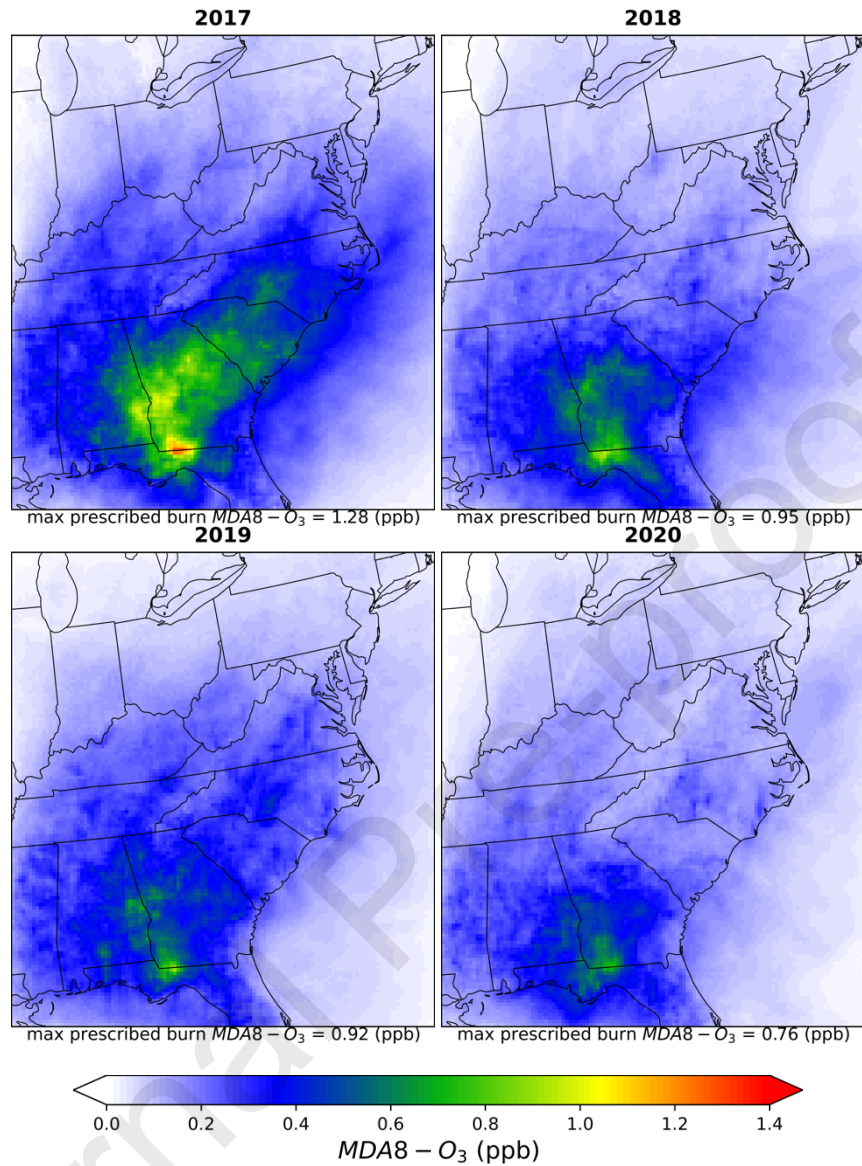
**Figure 1.** Spatial distribution of total prescribed burned area observed by adjusted-FINN (top) and corresponding total emissions of PM<sub>2.5</sub>, VOCs and NO<sub>x</sub> (bottom) during 2013–2020 (unit is acres for burned area and tons for PM<sub>2.5</sub>, VOCs and NO<sub>x</sub>) emissions.



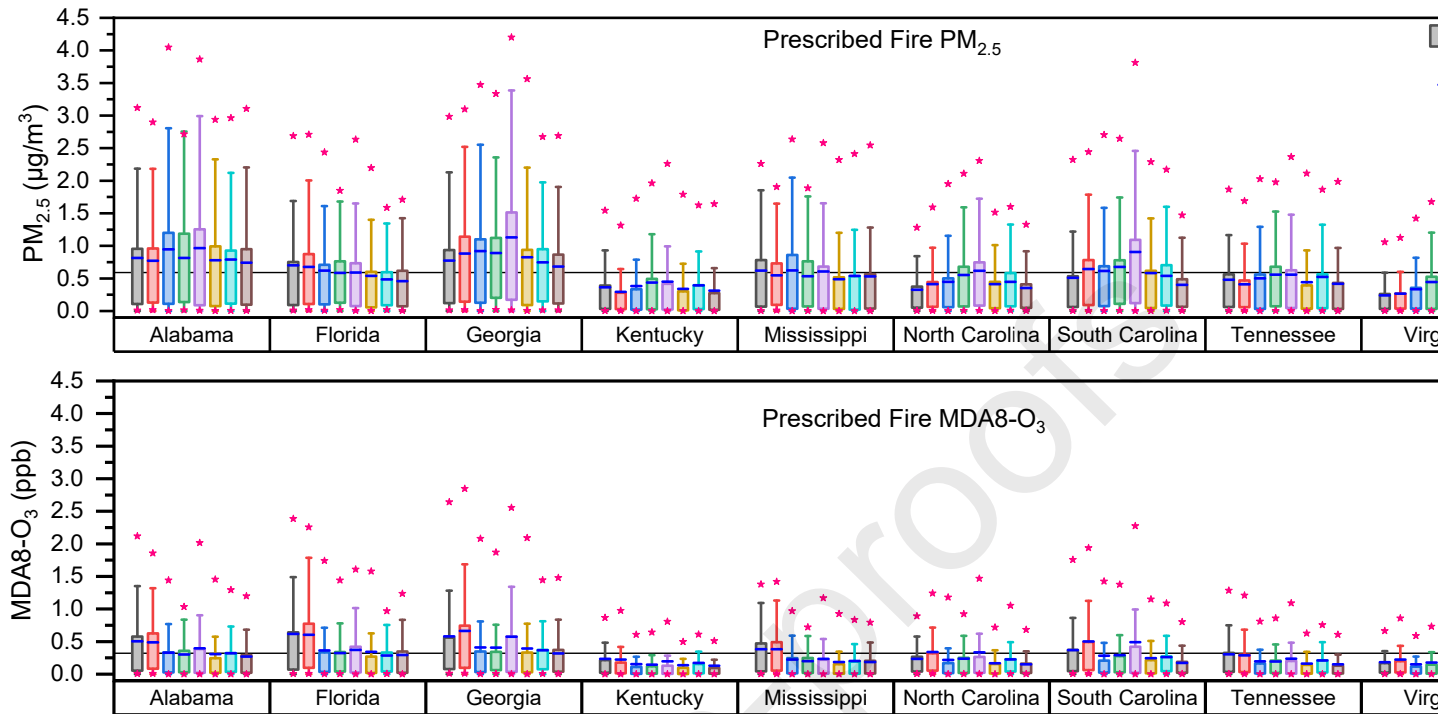


**Figure 2.** Spatial distributions of yearly average prescribed burn specific PM<sub>2.5</sub> concentrations ( $\mu\text{g}/\text{m}^3$ ) during 2013–2020.

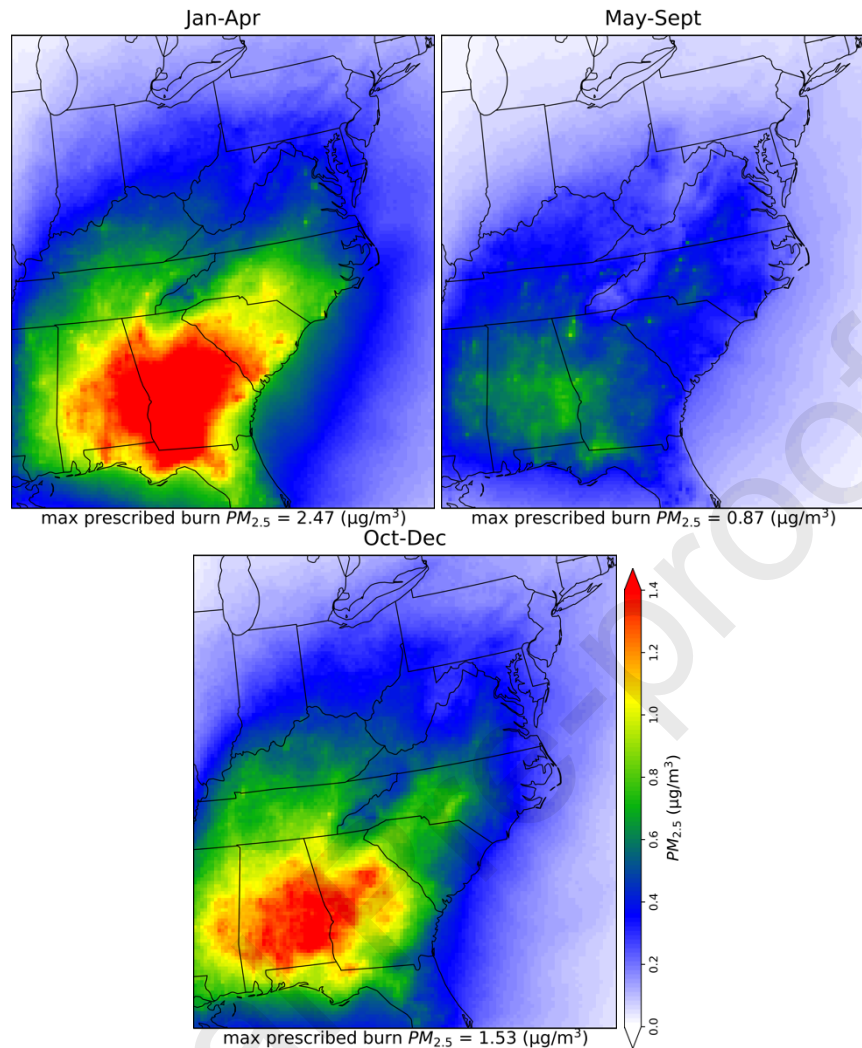




**Figure 3.** Spatial distributions of yearly average prescribed burn specific MDA8-O<sub>3</sub> concentrations (ppb) during 2013–2020.



**Figure 4.** Boxplot of state-specific prescribed burn contributed daily average  $\text{PM}_{2.5}$  (top panel) and daily  $\text{MDA8-O}_3$  (bottom panel) from 2013-2020. The top and bottom of the box indicate the 75<sup>th</sup> and 25<sup>th</sup> percentile of yearly values. The horizontal solid lines indicate the interquartile range of yearly values. The blue horizontal blue line is the annual mean and the top and bottom pink star indicate the 95<sup>th</sup> and 5<sup>th</sup> percentile of yearly values. The black horizontal long line indicates the average prescribed burn  $\text{PM}_{2.5}$  and  $\text{MDA8-O}_3$  over the study states from 2013-2020.



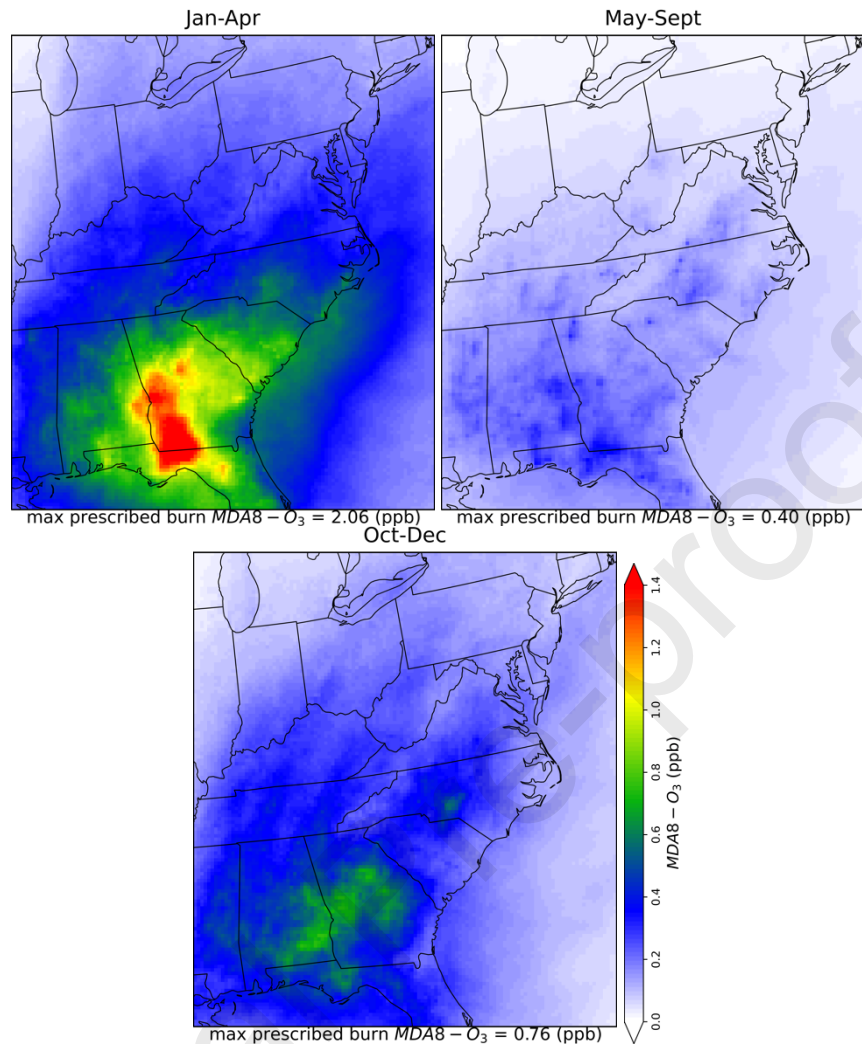


**Figure 5.** Spatial distributions of seasonal average prescribed burn specific PM<sub>2.5</sub> ( $\mu\text{g}/\text{m}^3$ ) (top row) and MDA8-O<sub>3</sub> concentrations (ppb) (bottom row) during 2013–2020. January–April is the extensive burning season, May–September is the low burning season and October–December is the moderate burning season.

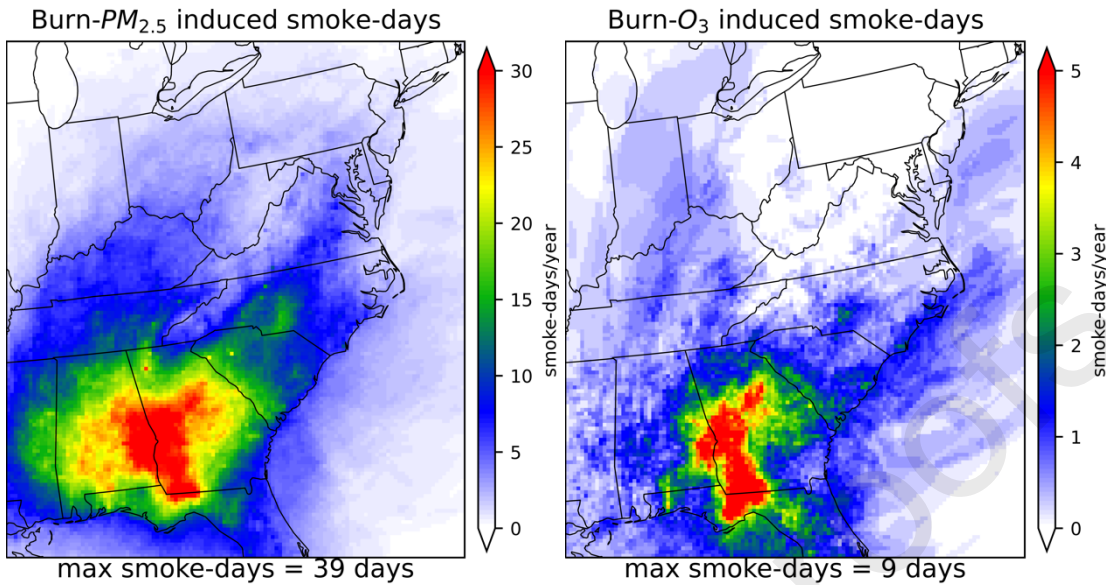


**Figure 6.** Distributions of the total smoke-days due to prescribed fire  $PM_{2.5}$  (left) and MDA8- $O_3$  (right) during 2013–2020. We defined a prescribed fire smoke-day as when prescribed burn smoke contributed  $\geq 10\%$  of NAAQS, i.e.,  $\geq 3.5 \mu\text{g}/\text{m}^3$  to 24-hr average  $PM_{2.5}$  mass concentration (NAAQS is  $35 \mu\text{g}/\text{m}^3$ ) and  $\geq 7 \text{ ppb}$  to MDA8- $O_3$  (NAAQS is 70 ppb).

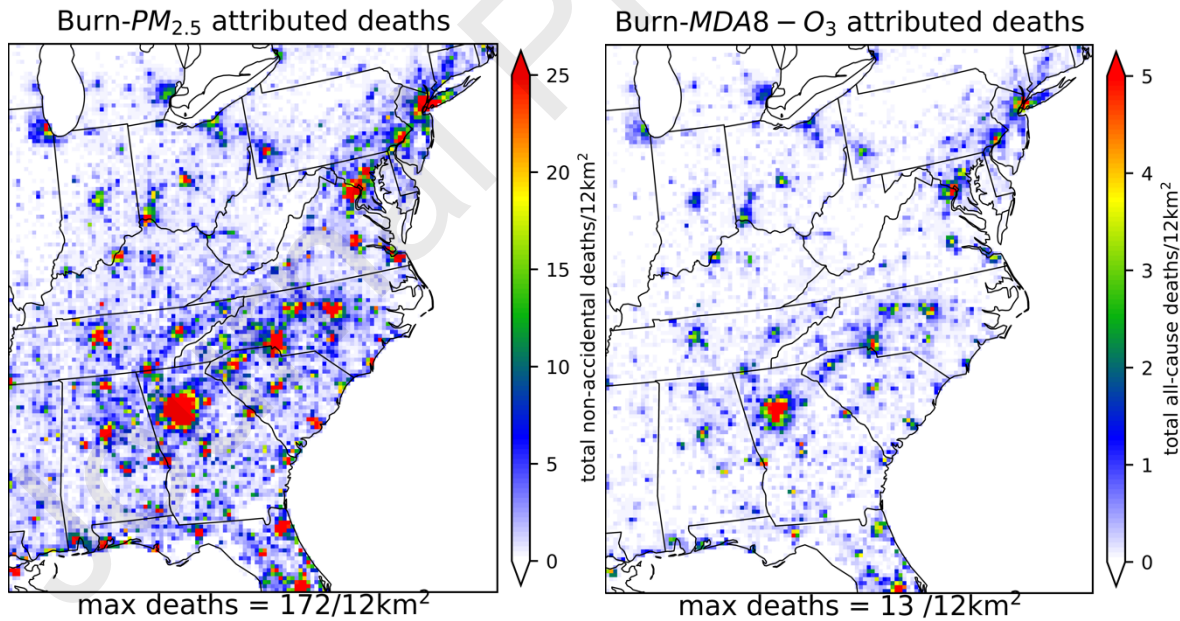


**Figure 7.** Distributions of premature mortality due to prescribed burn smoke  $PM_{2.5}$  exposure (left) and MDA8- $O_3$  exposure (right) at the gridded-level ( $12 \text{ km}^2$ ). The estimates of premature mortality are reported as the sum of annual values over 2013–2020. The

concentration-response relationship from GEMM-NCD+LRI was used for PM<sub>2.5</sub> and Sun et al. (2022) study for MDA8-O<sub>3</sub>.

**CRediT authorship contribution statement:**

KJM: conceptualization, data curation, formal analysis, software, visualization, writing – original draft, writing – review & editing. ZL& YH: data curation, formal analysis, investigation, software, writing – review & editing. AV, JDS & CM: resources, writing – review & editing. GW: funding acquisition, resources, investigation, writing – review & editing. PKL: resources, writing – review & editing. AGR: conceptualization, funding acquisition, methodology, resources, writing – review & editing. MTO: conceptualization, data curation, funding acquisition, investigation, resources, writing – review & editing.

**Declaration of interests**

The authors declare that they have no known competing financial interests or personal relationships that could have appeared to influence the work reported in this paper.